Environmental Protection Agency
An Ghníomhaireacht um Chaomhnú Comhshaoil

STRIVE
Report Series No.111

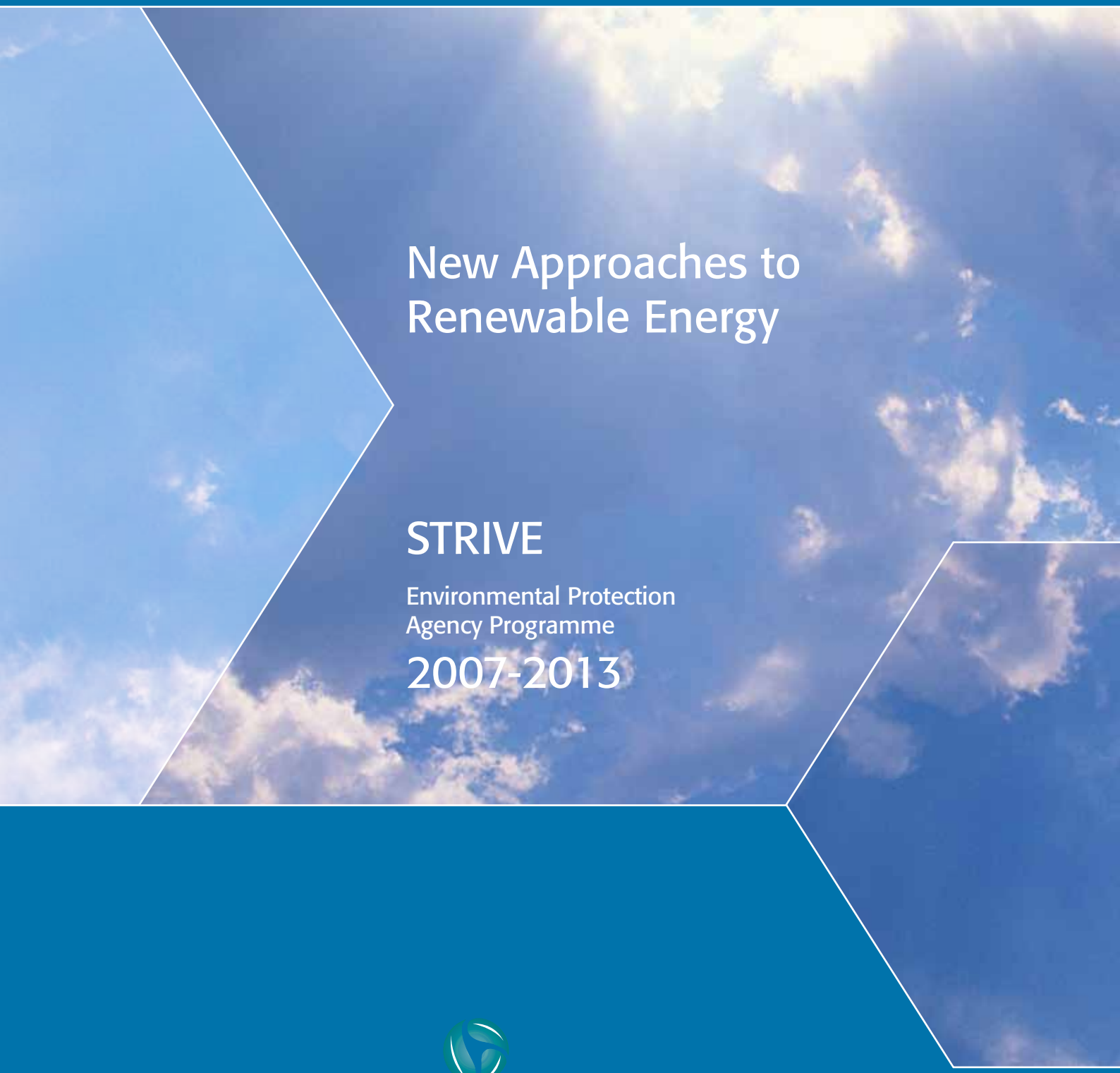

New Approaches to Renewable Energy

STRIVE

Environmental Protection Agency Programme

2007-2013

SSTI
Strategy for Science, Technology and Innovation

Comhshaol, Pobal agus Rialtas Áitiúil
Environment, Community and Local Government

Environmental Protection Agency

The Environmental Protection Agency (EPA) is a statutory body responsible for protecting the environment in Ireland. We regulate and police activities that might otherwise cause pollution. We ensure there is solid information on environmental trends so that necessary actions are taken. Our priorities are protecting the Irish environment and ensuring that development is sustainable.

The EPA is an independent public body established in July 1993 under the Environmental Protection Agency Act, 1992. Its sponsor in Government is the Department of the Environment, Community and Local Government.

OUR RESPONSIBILITIES

LICENSING

We license the following to ensure that their emissions do not endanger human health or harm the environment:

- waste facilities (e.g., landfills, incinerators, waste transfer stations);
- large scale industrial activities (e.g., pharmaceutical manufacturing, cement manufacturing, power plants);
- intensive agriculture;
- the contained use and controlled release of Genetically Modified Organisms (GMOs);
- large petrol storage facilities;
- waste water discharges;
- dumping at sea.

NATIONAL ENVIRONMENTAL ENFORCEMENT

- Conducting over 1200 audits and inspections of EPA licensed facilities every year.
- Overseeing local authorities' environmental protection responsibilities in the areas of - air, noise, waste, waste-water and water quality.
- Working with local authorities and the Gardaí to stamp out illegal waste activity by co-ordinating a national enforcement network, targeting offenders, conducting investigations and overseeing remediation.
- Prosecuting those who flout environmental law and damage the environment as a result of their actions.

MONITORING, ANALYSING AND REPORTING ON THE ENVIRONMENT

- Monitoring air quality and the quality of rivers, lakes, tidal waters and ground waters; measuring water levels and river flows.
- Independent reporting to inform decision making by national and local government.

REGULATING IRELAND'S GREENHOUSE GAS EMISSIONS

- Quantifying Ireland's emissions of greenhouse gases in the context of our Kyoto commitments
- Implementing the Emissions Trading Directive, involving over 100 companies who are major generators of carbon dioxide in Ireland.

ENVIRONMENTAL RESEARCH AND DEVELOPMENT

- Co-ordinating research on environmental issues (including air and water quality, climate change, biodiversity, environmental technologies).

STRATEGIC ENVIRONMENTAL ASSESSMENT

- Assessing the impact of plans and programmes on the Irish environment (such as waste management and development plans).

ENVIRONMENTAL PLANNING, EDUCATION AND GUIDANCE

- Providing guidance to the public and to industry on various environmental topics (including licence applications, waste prevention and environmental regulations).
- Generating greater environmental awareness (through environmental television programmes and primary and secondary schools' resource packs).

PROACTIVE WASTE MANAGEMENT

- Promoting waste prevention and minimisation projects through the co-ordination of the National Waste Prevention Programme, including input into the implementation of Producer Responsibility Initiatives.
- Enforcing Regulations such as Waste Electrical and Electronic Equipment (WEEE) and Restriction of Hazardous Substances (RoHS) and substances that deplete the ozone layer.
- Developing a National Hazardous Waste Management Plan to prevent and manage hazardous waste.

MANAGEMENT AND STRUCTURE OF THE EPA

The organisation is managed by a full time Board, consisting of a Director General and four Directors.

The work of the EPA is carried out across four offices:

- Office of Climate, Licensing and Resource Use
- Office of Environmental Enforcement
- Office of Environmental Assessment
- Office of Communications and Corporate Services

The EPA is assisted by an Advisory Committee of twelve members who meet several times a year to discuss issues of concern and offer advice to the Board.

EPA STRIVE Programme 2007–2013

New Approaches to Renewable Energy

New Approaches for the Generation of Hydrogen from Water Using Visible Light

(2008-ET-MS-3)

STRIVE Report

Prepared for the Environmental Protection Agency

by

Department of Chemistry, Dublin City University

Authors:

Mary Pryce, Han Vos, Jennifer Manton, Suraj Soman and Avishek Paul

ENVIRONMENTAL PROTECTION AGENCY

An Ghníomhaireacht um Chaomhnú Comhshaoil
PO Box 3000, Johnstown Castle, Co. Wexford, Ireland

Telephone: +353 53 916 0600 Fax: +353 53 916 0699
Email: info@epa.ie Website: www.epa.ie

ACKNOWLEDGEMENTS

This report is published as part of the Science, Technology, Research and Innovation for the Environment (STRIVE) Programme 2007–2013. The programme is financed by the Irish Government under the National Development Plan 2007–2013. It is administered on behalf of the Department of the Environment, Community and Local Government by the Environmental Protection Agency which has the statutory function of co-ordinating and promoting environmental research.

The Dublin City University group would like to acknowledge the steering committee: Prof. James Clarke (University of York, UK), Elaine Farrell (EPA) and Lisa Sheils (EPA) for all their invaluable input and help during the project.

DISCLAIMER

The EPA STRIVE Programme addresses the need for research in Ireland to inform policymakers and other stakeholders on a range of questions in relation to environmental protection. These reports are intended as contributions to the necessary debate on the protection of the environment.

EPA STRIVE PROGRAMME 2007–2013

Published by the Environmental Protection Agency, Ireland

ISBN: 978-1-84095-506-4

Price: Free **Online version**

Details of Project Partners

Dr. Mary Pryce
School of Chemical Sciences
Dublin City University
Dublin 9
Ireland
Tel.: +353 1 7008005
Email: mary.pryce@dcu.ie

Prof. Han Vos
School of Chemical Sciences
Dublin City University
Dublin 9
Ireland
Tel.: +353 1 7005307

Jennifer Manton
School of Chemical Sciences
Dublin City University
Dublin 9
Ireland

Suraj Soman
School of Chemical Sciences
Dublin City University
Dublin 9
Ireland

Avishek Paul
School of Chemical Sciences
Dublin City University
Dublin 9
Ireland

Prof. Sven Rau
Anorganische Chemie I
Universität Ulm
Albert-Einstein-Allee 11
89081 Ulm
Germany

Table of Contents

Executive Summary

Global climate change and security of energy supply are increasingly perceived as the most serious threats facing the world's medium and long-term future. This realisation has led to the establishment of a United Nations-driven Framework Convention on Climate Change and the Kyoto Protocol in 1997. It is clear that increasing carbon dioxide concentrations have the potential to seriously threaten life on earth as we know it now and novel methods to reduce carbon dioxide concentrations are needed. Therefore, European Union and G8 leaders agreed in 2009 that carbon dioxide emissions must be cut by 80% by 2050.

The most important property of any energy source is its environmental compatibility. Our current energy infrastructure is dominated by fossil fuel use, which leads to greenhouse gas emissions. One of the major challenges facing humanity is to develop a renewable source of energy to replace our dependence on fossil fuels. Ideally, this new source should be abundant, inexpensive, environmentally clean, and widely distributed geographically. Hydrogen is the third most abundant chemical element in the earth's crust. Currently, hydrogen is produced in large quantities from fossil fuels, which can be used in the short and medium term, but in the long term it is clearly unsustainable that the hydrogen economy is derived from hydrocarbons. To achieve the benefits of a truly sustainable hydrogen energy economy, hydrogen has to be produced from non-fossil fuel resources, such as water.

The 'hydrogen economy' is often mentioned as a solution since, as a fuel, hydrogen is non-polluting and does not produce carbon dioxide. The ultimate realisation of a hydrogen-based economy could potentially result in enormous environmental and economic benefits, together with enhanced security of energy supply. However, the transition from a carbon-based (fossil fuel) energy system to a hydrogen-based economy involves significant scientific, societal and technological barriers. Furthermore, to achieve the full environmental benefit of hydrogen as an energy carrier, low-carbon, low-polluting, and lower-cost processes for producing hydrogen from renewable energy sources must be developed. This project delivers such a technology, where hydrogen can be produced from water at room temperature and this brings us closer to a much desired green economy.

The utilisation of solar energy is high on the agenda in this respect since every hour about 4×10^{20} J of solar energy hit the earth, an amount roughly equivalent to the amount of energy consumed on the earth in a year. Photovoltaic cells producing electricity from sunlight have already been developed. The problem associated with voltaic cells, as with wind energy and tidal power, is that the energy generated cannot be stored and must be used when it is produced, also all three are intermittent.

One way around this is the 'solar fuel' approach, which aims to deliver a sunlight-driven and therefore environmentally friendly technology that can efficiently produce hydrogen from water or other fuels or chemical feedstocks from carbon dioxide. To achieve this, a light-absorbing centre was connected via a bridge to a catalytic centre that can generate hydrogen. This intramolecular approach was developed by a Dublin City University group in co-operation with German co-workers some years ago. It is envisaged that after absorption of light by the light-absorbing part of the assembly, an electron is transferred via the bridge to the catalytic centre where it is used to produce hydrogen from water.

Three different types of intramolecular complexes were prepared. Firstly, ruthenium and iridium-based light-absorbing centres were combined with hydrogen-evolving catalysts, such as palladium or platinum centres, using a range of bridging ligands. It was realised from the beginning of this project that the above-mentioned metals are expensive since they are not abundant, but this approach was necessary since the use of these metals allows for the development and understanding of the novel concepts needed to achieve the project goal. However, in the second phase of the project, second-generation compounds

based on abundant metals such as zinc and cobalt were investigated.

The results obtained in this project confirm that, when using this ‘biomimetic’ approach, hydrogen generation is observed. Importantly, it was shown as well that the technology developed can also be used to reduce carbon-dioxide-producing fuels such as carbon monoxide and formic acid, thus making it possible to recycle carbon dioxide into useful chemical products or fuels and so close the loop on a carbon-neutral economy. The systems developed need to be further optimised but the approach taken is clearly justified. By immobilisation of the compounds on active surfaces, such improvements can be obtained. Importantly, the compounds based on abundant metals also possess useful photoelectrocatalytic properties. The results obtained with this technique, where light as well as electricity is used, were very good and resulted in the efficient production of large amounts of hydrogen where the number of molecules produced per molecule of catalyst per hour is more than 10,000.

In conclusion, important first steps towards the development of a green approach to carbon dioxide reduction and recycling have been taken. In the Irish context, the development of the environment friendly production methods will provide employment and the potential for exporting this technology all over the world. Three major PhDs were produced from this research, demonstrating the ever-increasing technical and scientific expertise being built within Ireland’s research community. Further outputs will include peer-reviewed articles and patents. The work outlined in this report resulted in a critical mass of energy-related research expertise in the laboratories involved. At present, the further commercialisation of the results obtained is under way.

Therefore, if the full environmental benefit of hydrogen as an energy carrier is to be achieved, low-carbon-intensive, low-polluting, and lower-cost processes for producing hydrogen from renewable energy sources must be developed.

1 Introduction

Energy affects all aspects of modern life. It is an essential commodity for increasing productivity in both agriculture and industry. The world's energy requirements have been increasing due to our growing population, technological development, and higher living standards. Furthermore, reserves of fossil fuels will eventually not be able to meet our increasing energy demands. The most important property of any energy source is its environmental compatibility. Our current energy infrastructure is dominated by fossil fuel use, which leads to greenhouse gas emissions. One of the major challenges facing humanity is to develop a renewable source of energy to replace our dependence on fossil fuels. Ideally, this new source should be abundant, inexpensive, environmentally clean, and widely distributed geographically. Different renewable alternatives have been considered which may provide potential solutions to the current environmental issues. Renewable energy should be clean and inexhaustible. The most important benefit of a renewable energy system is a decrease in environmental pollution (Lewis and Nocera, 2006; McEvoy and Brudvig, 2006).

Of the few potential energy sources that might meet these criteria, sunlight is the most attractive. The sun delivers energy to the earth's surface at an average rate that is about four orders of magnitude greater than the current rate of worldwide technological energy use. Although practical methods for conversion of sunlight to electricity exist, solar-generated electricity currently does not compete successfully with that from fossil fuels. The diurnal nature of solar radiation, the fluctuation of sunlight intensity at the earth's surface as a function of the season and weather conditions, and the diffuse nature of solar energy, make it impractical for powering land vehicles. This in turn will necessitate either great advances in batteries or other devices for storing electricity, or the generation of fuels from sunlight, for example the generation of hydrogen from water using sunlight and then using it as a fuel (Ferreira et al*.,* 2004).

Hydrogen is potentially an ideal energy carrier, as it is non-polluting and gives up both its electrons upon oxidation to form only water. Although it is the most abundant element in the universe, elemental hydrogen is not present in great quantities on earth; most of the hydrogen present on earth is bonded to oxygen in the form of water. A number of challenges must be overcome for hydrogen to be used widely as a sustainable energy source. In order to achieve the full environmental benefit of hydrogen as an energy carrier, low-carbon intensive, low-polluting, and lower-cost processes for producing hydrogen from renewable energy sources must be developed. Scientific advances are needed to develop more energy-efficient and cost-effective methods for purification and delivery, and storage of hydrogen systems, especially for vehicular onboard storage, and to enable more durable fuel cells for converting hydrogen into electrical energy. The development of heterogeneous catalytic systems for hydrogen production from water under irradiation has been investigated during the last three decades. Intramolecular photocatalysts, however, are very attractive in the sense that their chemical and photochemical properties can be understood and tuned at the molecular level. Moreover, an intramolecular catalytic system may be covalently bound to a photosensitiser, which leads to more efficient electron transfer. Molecular devices for water splitting based on such systems are of great interest (Roeb et al*.,* 2009).

1.1 Solar Hydrogen – Fuel for the Future

Hydrogen can be obtained from diverse resources, both renewable (hydro, wind, wave, solar, biomass and geothermal) and non-renewable (coal, natural gas and nuclear). It can be stored as a fuel and used in transportation and distributed by heat and power generation systems using fuel cells, internal combustion engines or turbines, with the only by-product at the point of use being water. Hydrogen can also be used as a storage medium for electricity generated from intermittent, renewable resources,

such as solar, wind, wave and tidal power; it thereby provides the solution to one of the major issues of sustainable energy, namely the problem of intermittency of supply. The ability of hydrogen to replace fossil fuels in the transportation sector could address one of the world's major environmental problems (Jacobson et al., 2005). The importance of hydrogen as a potential energy carrier has increased significantly over the last decade, owing to rapid advances in fuel cell technology. Fuel cells, operating using hydrogen or hydrogen-rich fuels, have the potential to become major factors in catalysing the transition to a future sustainable energy system with low carbon dioxide (CO_2) emissions. Figure 1.1 illustrates the central role of hydrogen as an energy carrier, linking multiple hydrogen production methods and various end-user applications. One of the principal attractions of hydrogen as an energy carrier is obviously the diversity of production methods from a variety of resources. Hydrogen can be produced from coal, natural gas and other hydrocarbons by a variety of techniques, from water by electrolysis, photolytic splitting or high-temperature thermochemical cycles, from biomass and even from municipal waste. Such a diversity of production sources contributes significantly to the security of energy supply.

The conversion of solar energy into electricity or other forms of energy is a very promising way to solve the energy crisis problem. Since the total solar energy that reaches the earth's surface exceeds our total energy consumption by a factor of thousands, an attractive solution would be large-scale conversion of solar energy to electricity and fuel. Many attempts have been made to convert solar energy into electricity, especially after the discovery of new devices capable of utilising sunlight, i.e. dye-sensitised solar cells. Another way to utilise solar energy is water splitting, with the production of molecular hydrogen and oxygen. Molecular hydrogen is an ideal fuel because the only product of its combustion is water, when combustion is carried out in pure oxygen (Eisenberg and Nocera, 2005; Armaroli and Balzani, 2007). Many studies on visible light-driven water splitting into hydrogen with either heterogeneous or homogeneous systems have been reported since the late 1970s, including studies by Lehn and Sauvage (1977), Kalyanasundaram et al. (1978) and Grätzel (1981). The key components of these photochemical hydrogen-evolving systems are usually a light-harvesting photosensitiser, a sacrificial electron donor, and a proton-reduction catalyst. With the aim of developing light-driven hydrogen-evolving devices, several photo-induced molecular devices for

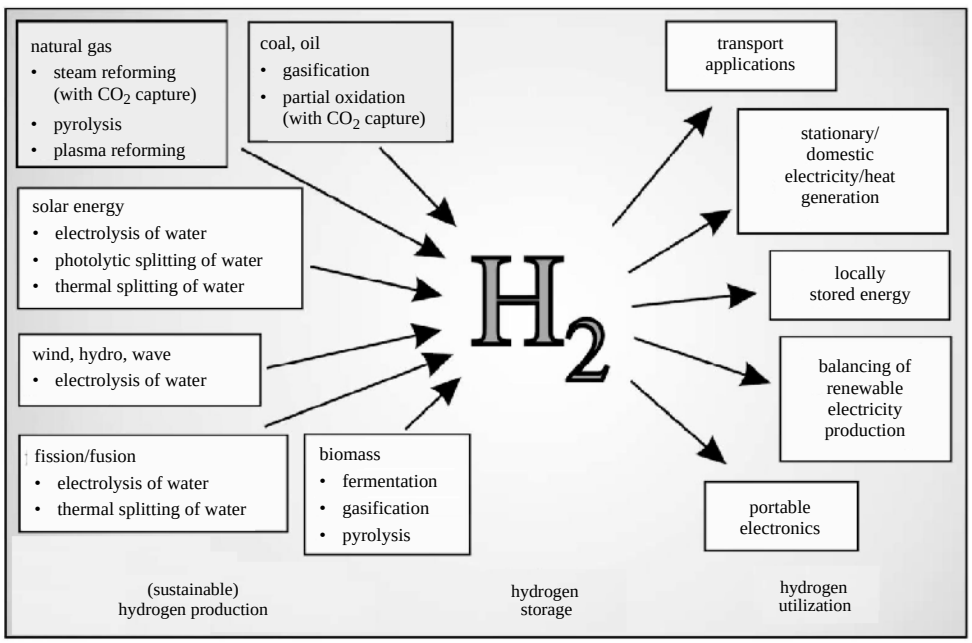

Figure 1.1. Hydrogen as an energy carrier linking multiple hydrogen production methods, through storage to various end-users (derived from Edwards et al. (2007)).

homogeneous hydrogen generation were constructed in recent years, including devices proposed by Esswein and Nocera (2007) and Rau et al. (2007). Solar energy stored in hydrogen is available at any time and at any place on earth, regardless of when or where the solar irradiance (or the hydropower, biomass, ocean energy or wind energy) was converted. The fundamental discrepancies in the times and places of solar energy supply and human energy demands can be overcome using hydrogen. Solar hydrogen combines the advantages of hydrocarbons with the those of solar energy (ecological acceptability, renewability and low risk).

A typical energy chain for hydrogen will comprise hydrogen production, distribution and delivery through hydrogen storage and ultimately its utilisation. The energy chain for sustainable hydrogen energy will involve the harvesting of sunlight or other energy sources to yield hydrogen as the energy carrier, and the storage and distribution of this energy carrier to its utilisation at an end device centred on either fuel cells or combustion, where it is converted to power. The ultimate realisation of a hydrogen-based economy could potentially confer enormous environmental and economic benefits, together with enhanced security of energy supply. Perhaps, the most telling argument for a sustainable hydrogen economy is the potential (globally) to drastically reduce carbon emissions. However, the transition from a carbon-based (fossil fuel) energy system to a hydrogen-based economy involves significant scientific, technological and socio-economic barriers to the implementation of hydrogen as the clean energy source of the future (Rodat et al., 2010).

1.2 Main Approaches for Hydrogen Production

Hydrogen is the third most abundant chemical element in the earth's crust, but it is invariably bound in chemical compounds with other elements. It must, therefore, be produced from other hydrogen-containing sources using energy, such as electricity or heat. At present, hydrogen is produced in large quantities from fossil fuels by steam reforming of natural gas and partial oxidation of coal or heavy hydrocarbons (Sigfusson, 2007). These methods can take advantage of economies of scale and are currently the cheapest and most established techniques for the large-scale production of hydrogen. They can be used in the short to medium term to meet hydrogen fuel demand and enable the production and testing of technologies related to hydrogen production, storage, distribution, safety and use. However, in the long term, it is clearly unsustainable that the hydrogen economy is driven by hydrogen derived from hydrocarbons. Moreover, to achieve the benefits of a truly sustainable hydrogen energy economy, hydrogen has to be produced from non-fossil resources, such as water (Turner, 2004; Sherif et al., 2005; Penner, 2006). Hydrogen can be produced by splitting water through various processes, including electrolysis, photo-electrolysis, high temperature decomposition and photo-biological water splitting. The commercial production of hydrogen by electrolysis of water achieves an efficiency of 75% but the cost is currently several times higher than that produced from fossil fuels. Electricity derived from renewable energy resources (e.g. wind, wave, tidal) might provide local hydrogen needs, but it will not meet the volumes of hydrogen required globally for its widespread use as the new energy source (Ewan and Allen, 2005).

Among the different approaches, solar energy has received much attention as a possible method for photochemical conversion and storage of solar energy. Photosynthetic bacteria represent a method with appreciable efficiency for hydrogen evolution using solar energy. The various renewable pathways for hydrogen production from solar energy are shown in Fig. 1.2.

Achieving low-cost and efficient solar energy production of hydrogen requires the development of innovative materials, emerging physical phenomena, novel synthetic techniques and new design concepts. Some of the main technologies used for hydrogen production and their status of development are discussed in the following sections.

1.2.1 Electrochemical processes

Water electrolysis is one of the most important industrial processes for hydrogen production today, and is expected to become even more important in the future. The three major technologies currently under

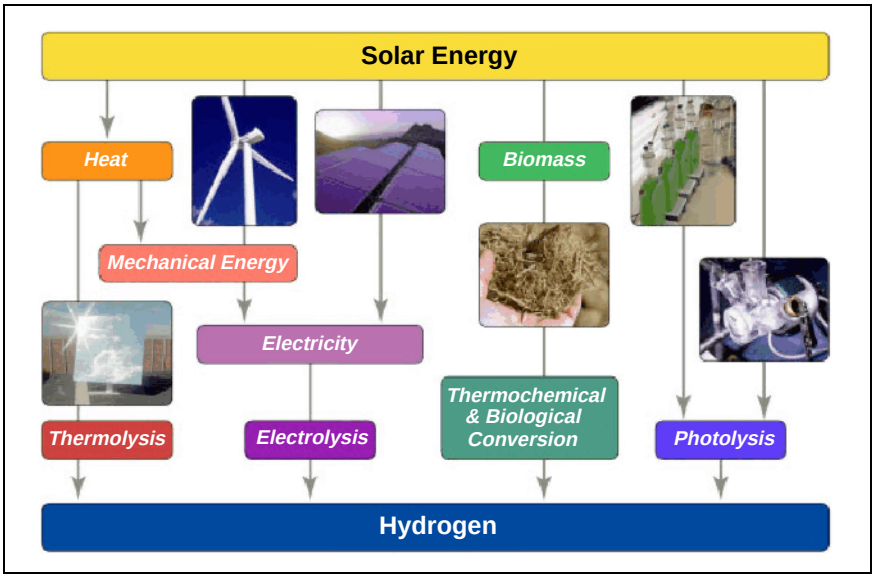

Figure 1.2. Renewable pathways for hydrogen production (derived from Turner et al. (2008)).

consideration for electrolytic hydrogen production are classified as alkaline, polymer membrane and ceramic oxide electrolyte. Developments of solid electrolytes for water electrolysis at intermediate temperatures are also important as illustrated by Linkous (1992). A principal focus of modern research in hydrogen production by electrolysis is to discover electrode materials that exhibit good electrochemical stability and show interesting activity for the typical electrochemical reactions. It is also desirable that these materials be inexpensive, abundantly available, easy to manipulate and non-polluting.

1.2.2 Photochemical processes

Hydrogen production by solar energy is via the direct photochemical reduction of water. Of the various possible methods, nature provides a blueprint for converting solar energy in the form of chemical fuels (Nelson and Shem, 2004). A leaf is a synergy of elaborated structures and functional components in order to produce the highly complex machinery for photosynthesis in which light harvesting, photo-induced charge separation, and catalysis modules combine to capture solar energy and split water into oxygen and 'hydrogen' efficiently. In artificial photocatalytic systems, the photosensitiser is excited by visible light and can thereafter effect redox reactions, yielding electrons for the water reduction. One of the benefits of this system is that several sensitisers with different absorption characteristics can be used simultaneously, leading to higher quantum yields per unit area. Thus, the design of efficient, cost-effective artificial systems by the coupling of leaf-like hierarchical structures and analogous functional modules under the guidance of the key steps of natural photosynthesis would be a major advance in the development of materials for energy conversion.

1.2.3 Photocatalytic hydrogen production

Photocatalytic water splitting employs light and semiconductors to split water. This process will be advantageous for the large-scale application of solar hydrogen production because of its simplicity. Water splitting using light energy has been studied for a long time using powder and electrode systems since the Honda–Fujishima effect was initially reported by Fujishima and Honda (1971) and completed by them in 1972 (Fujishima and Honda, 1972). There is no doubt that photocatalytic water splitting will contribute to green sustainable chemistry. The final target of this research field is to achieve artificial photosynthesis and solar hydrogen production from water. The main processes in a photocatalytic reaction are:

- Absorption of photons to form electron–hole pairs;
- Charge separation and migration of photogenerated carriers; and
- Chemical reactions.

Water splitting proceeds on heterogeneous photocatalysts using semiconductor materials. Semiconductors have the band structure in which the conduction band (CB) is separated from the valence band (VB) by a suitable band gap. Irradiation results in the generation of electrons and holes in the CBs and VBs, respectively. The photogenerated electrons and holes cause redox reactions similarly to electrolysis. Water molecules are reduced by the electrons to form hydrogen and are oxidised by the holes to form oxygen (for overall water splitting).

1.2.4 Biomemetic hydrogen production

Photosynthetic green algae and cyanobacteria provide a promising pathway for generating hydrogen on a large scale. Green algae and cyanobacteria can use solar energy to convert water into hydrogen gas, an energy carrier whose use does not emit greenhouse gases (Singh et al., 1990). Hydrogen production by these microorganisms depends on the availability of plentiful resources, namely water as a substrate and solar energy as the energy source. Moreover, the oxygen and hydrogen that such cells produce could be used in a fuel cell to generate electricity.

Green algae and cyanobacteria absorb light through pigments that are associated with two photosystems, photosystem I (PSI) and photosystem II (PSII). The absorbed light energy is transferred from the antenna pigments to the chlorophyll reaction centre molecules where charge separation occurs, yielding oxidants and reductants. PSI generates a reductant that eventually reduces the iron-sulfur protein ferredoxin, which plays several roles. Its main function is to provide electrons to generate nicotinamide adenine dinucleotide phosphate (NADPH) via ferredoxin-NADP oxidoreductase. NADPH, along with adenosine triphosphate (ATP), is needed for fixing carbon dioxide and for producing carbohydrates. However, in the absence of carbon dioxide and under anaerobic conditions, reduced ferredoxin or NADPH reduces protons to yield hydrogen gas, a reaction catalysed by hydrogenase. Ferredoxin links photosynthetic electron transport directly to hydrogen production in green algae, whereas NADPH is the likely electron donor to hydrogenase in cyanobacteria.

Inspired by nature, the authors developed a biomimetic approach, where a range of compounds was prepared, containing one unit to absorb light and one that acts as a catalyst to produce hydrogen (or reduce carbon dioxide), mimicking what happens in the photosynthetic centres in nature. It was envisaged that for these, intramolecular, systems after absorption of light by the photosensitiser part of the assembly, an electron would be transferred to the catalytic centre where the electron would be used to reduce water to hydrogen. The results obtained confirm that hydrogen is indeed obtained in this manner. Three different types of intramolecular complexes were prepared. In the first series, an iridium (Ir) light-absorbing centre is combined with hydrogen-evolving catalysts such as palladium (Pd) or platinum (Pt) centres using a range of bridging ligands. Secondly, ruthenium (Ru) complexes were used as photosensitisers and were combined with catalytic rhenium (Re) centres using a similar approach. It was realised from the beginning of this project that the above-mentioned metals are very expensive since they are not abundant. It was therefore decided in the third part of this study to also develop systems based on abundant metals such as cobalt (Co) and zinc (Zn).

A large aspect of the project involved the synthesis and characterisation of the various compounds. The characterisation included the verification of the structural features of the compounds using techniques such as nuclear magnetic resonance (NMR), electronic spectroscopy and elemental analysis. The photocatalytic measurements for the Ir/Pd and Ir/Pt assemblies showed considerable amounts of hydrogen. These amounts were dependent on the reaction conditions, in particular the amount of water present. Surprisingly, the best results were obtained by the use of visible light, even though the iridium component absorbed weakly in the visible part of the electronic absorption spectrum. It was also noted that the results observed are dependent on the type of bridging ligand used to bring the light-absorbing centre and the catalyst together. This clearly shows that the hydrogen generation of the compounds depends directly on the electronic properties of the molecular components and the amounts of hydrogen produced justify the intramolecular approach taken.

Some unexpected results were obtained for the Ru/Re assemblies. Rhenium can act as a catalytic centre for the photocatalytic generation of hydrogen but the reduction of carbon dioxide has also been observed. For the compounds investigated in this project, only an activity towards carbon dioxide was observed. Under the normal 'hydrogen' experimental conditions, no hydrogen was observed, but in the presence of carbon dioxide both carbon monoxide (CO) and formic acid were observed. This is an important observation since it shows that with the approach taken carbon dioxide can be recycled into high-energy compounds for energy applications.

Finally, a series of cobalt and porphyrin compounds were investigated as examples of low-cost photocatalysts. The photocatalytic experiments carried out with these compounds were somewhat disappointing but the photoelectrocatalytic approach proved very promising. In the photoelectrocatalytic studies, ~10,000 molecules of hydrogen per molecule of catalyst were obtained.

2 Photocatalysis Using Cyclometallated Iridium (III) Complexes

In the following sections the results obtained are reviewed. Synthetic aspects, as well as the electronic properties, of the iridium, ruthenium and cobalt-based compounds are outlined and their catalytic properties are discussed.

2.1 Mononuclear Ir Complexes for Intermolecular Photocatalytic H_2 Generation

As reported by Kalyanasundaram (1992), as a consequence of greater ligand field stabilisation energy (LFSE), the use of cyclometallated iridium (III) complexes avoids the thermal population and subsequent non-radiative decay from the dissociative triplet metal-centred (^{3}MC) state observed in tris-diimine ruthenium (II) complexes. In addition, the greater energetic requirements for the population of the ^{3}MC state allow a larger range of excited state energies by altering the ligand architecture, as illustrated by Watts and Van Houten (1974). The 'tuning' of the excited state properties of the $[Ir(C^N)_2(N^N)]^+$ complex is further facilitated by the formation of a mixed excited triplet state associated with metal-to-ligand charge transfer (MLCT), ligand centred (LC) transitions and ligand-to-ligand centred transitions (LLCT), respectively (Colombo et al., 1993, 1994; Hay, 2002).

To facilitate the transfer of reducing equivalents, an electron relay such as methyl viologen is typically employed. The choice of an electron relay is generally crucial to the success of a system; a good relay oxidatively quenches the excited photosensitiser, thereby creating charge separation. Numerous relays have been used in place of methyl viologen, including a variety of quaternary bipyridines, as shown by Amouyal et al. (1980) as well as several cobalt (Krishnan and Sutin, 1981; Hawecker et al., 1983a,b; Krishnan et al., 1985) and rhodium (Brown et al., 1979; Kirch et al., 1979; Chan et al., 1981) complexes. Ozawa et al. (2006) and Rau et al. (2006) have proposed alternatives that include bridged systems where a photosensitiser is covalently linked to a hydrogen-evolving metal complex. Aside from net energy loss, the use of an electron relay allows charge separation at the expense of simplicity, which is compounded by the presence of a sacrificial electron donor that allows hydrogen evolution without concurrent water oxidation.

The first mononuclear iridium-based intermolecular catalytic system described by Bernhard and co-workers (Goldsmith et al., 2005) and which uses only a molecular photosensitiser (PS), colloidal metal catalyst, sacrificial reductant (SR), and visible light to evolve substantial amounts of hydrogen in the absence of an electron relay species is shown in Fig. 2.1 (Constable and Seddon, 1982; Esswein and Nocera, 2007; Rau et al., 2007).

Systems that do not have an electron relay, while advantageous, are uncommon in the literature (DeLaive et al., 1979). It has been reported by Rau et al. (2007) that unlike $[Ru(bpy)_3]^{2+}$ (bpy, 2,2'-bipyridine), heteroleptic cyclometallated iridium (III) complexes, such as the $[Ir(ppy)_2(bpy)]PF_6$ (ppy, 2-phenylpyridine) photosensitiser used, are directly quenched by sacrificial electron donors such as triethylamine (TEA) and triethanolamine (TEOA). Goldsmith et al. (2005) found that quenching of the PS creates an activated reduced species capable of

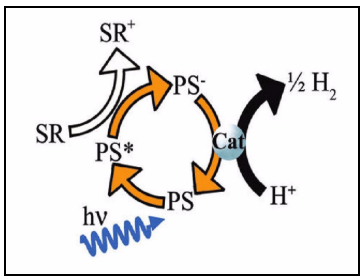

Figure 2.1. General reaction pathways for mononuclear intermolecular catalytic systems (derived from Esswein and Nocera (2007)). PS, photosensitiser; SR, sacrificial reductant.

independently reducing protons or delivering reducing equivalents to catalytic centres to evolve hydrogen. Such a system that avoids an electron relay is inherently simpler. In addition, energy losses and back reactions associated with the electron transfer to the relay are eliminated, while coupling of the PS to the water redox couple is facilitated.

2.2 Binuclear Ir Complexes for Intramolecular Photocatalytic H_2 Generation

The central processes in natural photosynthesis are light-driven electron transfer from the special pair chromophores to the primary acceptor, and the subsequent charge separation to enable the reduction of substrates. The transfer of these design principles to artificial systems has led to the development of catalytic multi-component systems for photocatalytic hydrogen production (Edwards et al., 2007) and carbon dioxide reduction (Hawecker et al., 1983a,b). In these systems, active metal complexes and catalysts are used to facilitate photo-induced electron transfer. For example, Kalyanasundaram et al. (1978) showed that heterogeneous photocatalytic systems can be used for the generation of hydrogen, and Currao et al. (2004) reported the photochemical splitting of water with a system consisting of a photoactive silver/silver chloride anode and a silicon solar cell acting as a cathode. However, in these heterogeneous systems, the electron transfer processes depend on many interfacial parameters that are difficult to influence.

It should be easier to control vectorial photoelectron transfer in an intramolecular photocatalyst by precise tuning of the physical properties and orientation of the molecular components. If it were also possible to slow down charge recombination processes, efficient photocatalytic systems may become feasible. A range of intramolecular photocatalysts were reported in the literature but most of them use a ruthenium metal centre as the light-absorbing unit, with only a few examples of iridium intramolecular systems reported so far, including the Ir–Co systems by Fihri et al. (2008a,b) and Andreiadas et al. (2011) and the self-assembled Ir–Co systems by Jasimuddin et al. (2010). For the reported intramolecular iridium systems, the efficiency is relatively low, with turnover numbers (TONs) of less than 50. This shows the need for improved systems with this metal using different peripheral ligands, bridging ligands and catalytic centres. A series of heterodinuclear Ir–Pt/Pd systems with various peripheral ligands and bridging units was made, all of which proved to be more efficient in producing hydrogen compared with the conventional Ru–Pt/Pd systems currently available (Watts and Van Houten, 1974; Ozawa et al., 2006). The heterodinuclear Ir–Pt/Pd photocatalyst consists of the following three components as shown in Fig. 2.2.

1. An iridium (III) fragment acting as the light absorber (Dietzek et al., 2006);

2. A $PtCl_2/PdCl_2$ unit which, when co-ordinated at the other end of the assembly, acts as a catalytic centre; and

3. A bridging unit (bpp, dpp, tpy, bpm, etc.) connecting the two metal centres through a conjugated reducible π-electron system (Chiorboli et al., 2003).

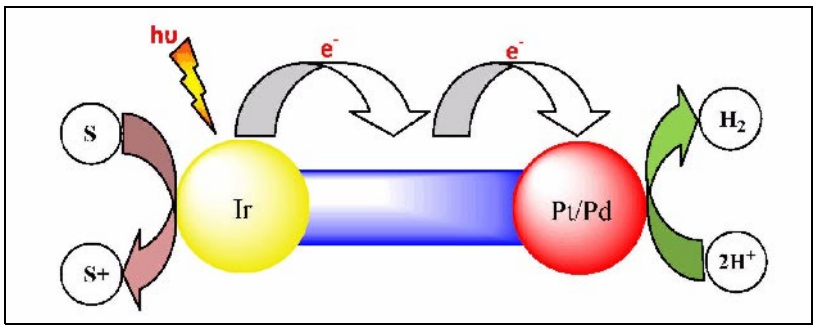

Figure 2.2. General reaction pathway for a heterodinuclear intramolecular photocatalytic system. S, sacrificial agent.

In the first step of the photocatalytic process, the iridium moiety is excited using both visible (470 nm) and ultraviolet (UV) (350 nm) light. To facilitate efficient electron transfer to the Pt/Pd centres, the TEA electron donor was utilised to re-reduce the photochemically formed iridium (IV) centres. The electron reaching the Pd/Pt catalytic centres reduces the proton to form hydrogen.

2.3 Role of Bridging Ligand

The ligand chosen to bridge the two metal centres is of vital importance because, as has been discussed previously, electronic communication is fundamental for the intramolecular photocatalyst to function properly. The ligands chosen here are (2-(6-(pyridin-2-yl)pyridin-3-yl)pyridine) (bpp) and 2,5-di(pyridin-2-yl)pyrazine (dpp), 2,2:6,2-terpyridine (tpy) and 2,2-bipyrimidine (bpm) as shown in Fig. 2.3. These ligands are good starting blocks as their electronic communication between different metal centres such as Ru–Pt/Pd, Ru–Os, Ru–Ru, has been extensively studied by Singh Bindra et al. (2011), Shultz et al. (2011) and Losse et al. (2010).

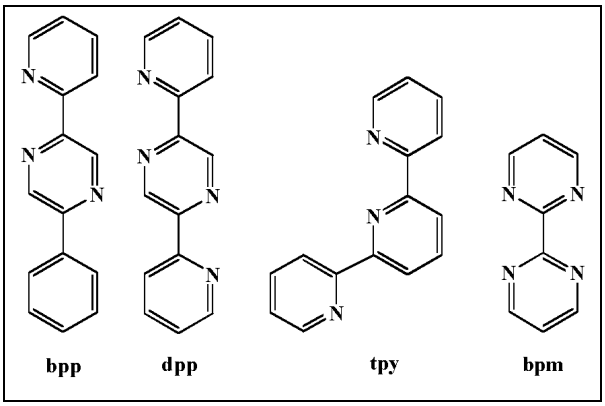

Figure 2.3. The structures of the bridging ligands employed in this section.

2.4 Ir Complexes Investigated

This aspect of the research project focuses on the synthesis, characterisation, photophysics and photocatalysis of cyclometallated iridium (III) complexes and novel complexes with bridging ligands bpp, tpy, bpm, and dpp. A small library of 25 cyclometallated iridium (III) complexes was synthesised and investigated for their potential to produce hydrogen photocatalytically. These complexes were characterised in full with the help of one and two-dimensional NMR spectroscopy. Deuteriation was used in spectroscopic characterisation and to probe the excited state electronic structure. Deuteriation studies included absorption, emission and lifetimes of cyclometallated iridium (III) complexes of the type $[Ir(N\hat{}C)_2(N\hat{}N)]^+$ where deuteriation was carried out on N^N neutral ligands. These types of deuteriated iridium (III) complexes have not been reported previously. Studies and measurements showed that iridium metal complexes can act as excellent catalytic systems for photogeneration of hydrogen, having efficiencies much higher than other metals such as ruthenium. For intramolecular catalytic hydrogen generation, an efficient light-absorbing unit and a bridging ligand that can transfer electrons to the catalyst from the light-absorbing unit are required, together with an efficient metal catalyst that can use the electrons in order to reduce water to produce hydrogen. A series of iridium cyclometallated precursors were synthesised for using as photosensitisers.

The first of its kind of heterodinuclear Ir–Pt/Pd photocatalytic system complexes investigated by the authors of this report was recently published. And, interestingly, these complexes have their second metal (Pt/Pd) attached to the bridging ligand in a cyclometallated manner. Basic photophysical measurements, including absorption, emission and lifetimes for all these complexes, were performed, which showed that, with this range of cyclometallated iridium (III) complexes, it was possible to tune the emission over the entire range of the visible spectrum by varying the substituents on the peripheral ligands, and the neutral chelating ligands. This has potential application for organic light-emitting diode (OLED) devices, which were not discussed in this report. All of the complexes presented in this report are promising candidates for photocatalytic hydrogen production, and gave good TONs that are comparatively higher than those produced by the analogous ruthenium complexes. Both intermolecular and intramolecular photocatalysis produced hydrogen, but intramolecular proved to be more efficient than intermolecular photocatalysis. Of the intramolecular systems, the Ir–Pt systems showed better catalytic activity than the Ir–

Pd systems, possibly due to the photophysical measurements. Time-dependent photocatalysis gave an idea of the efficiency of these novel photocatalysts. Also, the ester complexes produced almost double the hydrogen than the non-ester complexes in solution. One of the interesting studies presented is a comparison of photocatalysis using visible (470 nm) and UV light (350 nm). The higher efficiency of 470 nm excitation, in conjunction with the photophysical data, suggests that the ^{3}MLCT state plays a crucial role in intramolecular photocatalysis of Ir–Pt/Pd heterodinuclear complexes.

A schematic representation of the entire range of complexes discussed in this report is presented in Fig. 2.4.

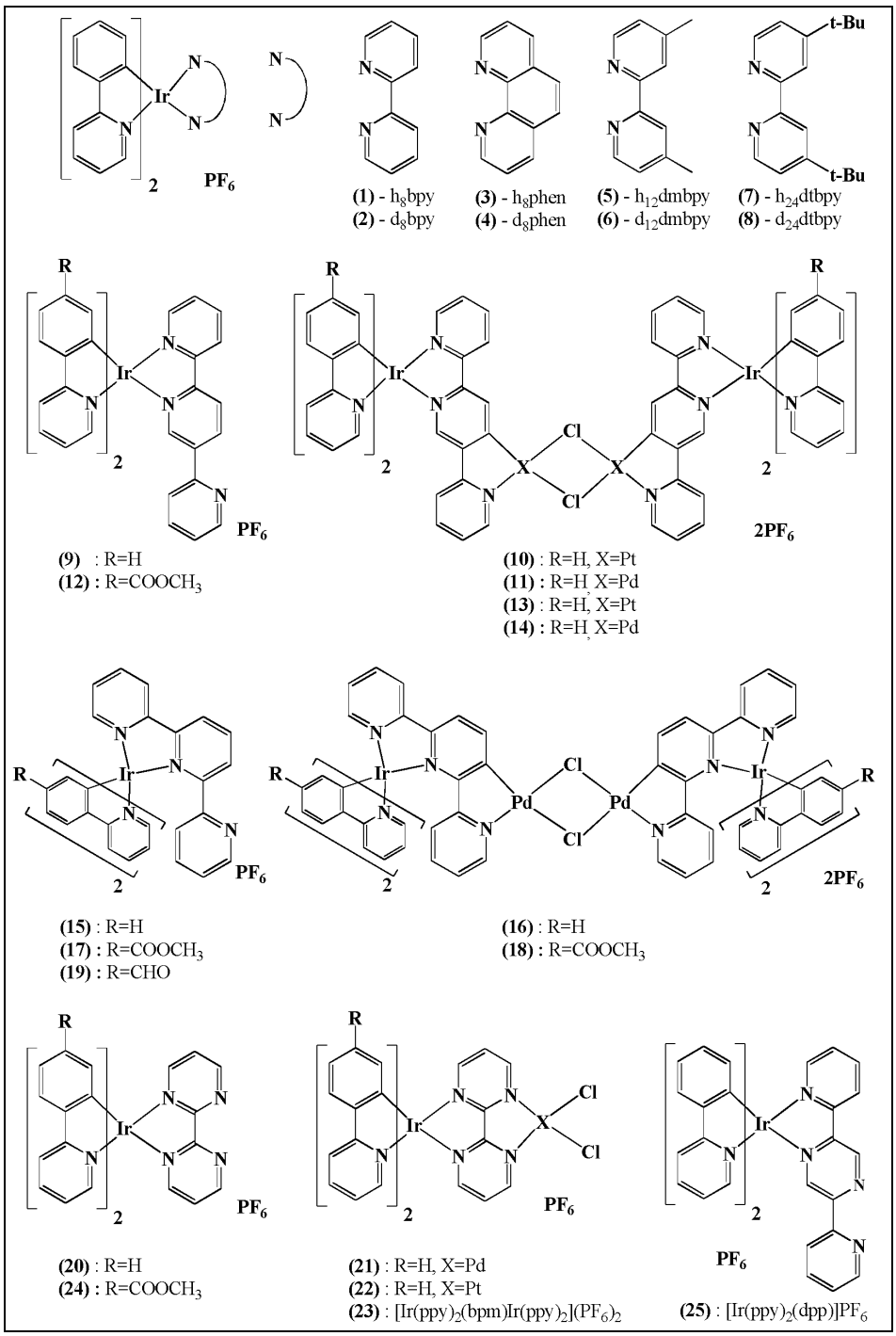

Figure 2.4. Schematic representation of the complexes discussed in this report.

2.5 Synthesis

For the synthesis of the iridium mononuclear complexes, two different reaction methods were used, both of which worked well. One method involved refluxing the dichlorobridged dimer $[Ir(ppy)Cl]_2$ with the N^N ligands (bpy, $d_8$bpy, phen, $d_8$phen, dmbpy, d_{12}dmbpy, dtbpy, d_{24}dtbpy) in ethylene glycol at 150°C, precipitation with potassium hexafluorophosphate (KPF_6) and purification by recrystallisation. The second method involved refluxing $[Ir(ppy)Cl]_2$ with the N^N ligands in a dichloromethane/ethanol (DCM/EtOH) (3:1) mixture, precipitation by KPF_6 and purification by recrystallisation from an acetone/water mixture. The synthesis of the mononuclear and heterodinuclear (Ir–Pt/Pd) iridium complexes with ligand bpp is explained below. The synthesis of the mononuclear complexes was carried out in a DCM/EtOH (3:1) mixture. Care was taken in adding the dichlorobridged dimer complex to the ligand (the precursor dissolved in the same solvent mixture was added drop-wise in a 2-h time interval). For the heterodinuclear Ir–Pt complexes, the mononuclear iridium complexes **(9)** and **(12)** were reacted with potassium tetrachloroplatinate(II) (K_2PtCl_4) in methanol under reflux. This reaction has to be done carefully with a minimum amount of solvent and the temperature of 105°C has to be kept constant throughout the entire reaction. The reaction for **(10)** requires 24 h for completion and **(13)** requires 48 h; afterwards the formed complex is filtered, washed with excess methanol and recrystallised from an acetone/diethylether (2:1) mixture two to three times. The same method was used for the reaction of these monomers with ammonium tetrachloropalladate(II) ($(NH_4)_2PdCl_4$) to obtain compounds **(11)** and **(12)**.

The synthesis of the mononuclear and heterodinuclear (Ir–Pt/Pd) iridium complexes with the ligand tpy as outlined below. The mononuclear complexes **(15)**, **(17)** and **(19)** were synthesised according to the method explained above. The reaction was carried out in a DCM/EtOH (3:1) mixture. Care was taken in the addition of the dichlorobridged dimer complex to the ligand. The product was recrystallised from an acetone/water (2:1) mixture. The reaction of these mononuclear precursors with K_2PtCl_4 was tried using a similar method to that outlined for complexes **(10)** and **(13)**. But, unfortunately, even by changing the reaction conditions (solvent, temperature and reaction time), the reaction did not work. One reason might be that the steric strain as the tpy ligand has one pyridine ring attached to the sixth position of the middle pyridine ring which might be causing some problem for complexation of platinum. But both the monomers undergo reaction with $(NH_4)_2PdCl_4$ and it was possible to isolate pure products. For complex **(16)** the reaction time was 24 h whereas for complex **(18)** it was 48 h, both at reflux.

The synthetic details of the mononuclear, homodinuclear (Ir–Ir) and heterodinuclear (Ir–Pd/Pt) iridium complexes **(20)**, **(21)**, **(22)**, **(23)** and **(24)** with the bpm ligand as outlined below. Synthesis of the mononuclear complexes **(20)** and **(24)** uses the same procedure as explained above for bpp and tpy ligands. The only change made was the solvent mixture, methanol (MeOH), was used instead of EtOH. Care has to be taken in adding $[Ir(ppy)_2Cl]_2$ dissolved in DCM to the bpm ligand dissolved in a DCM/MeOH (2:1) solvent mixture as the possibility of dimer formation is very high for these complexes. For the Ir–Pd dinuclear complex **(21)**, the mononuclear complex **(20)** was reacted with $[Pd(ACN)_2Cl_2]$ in acetonitrile (ACN). The reaction was complete after 6 h reflux. Precipitation by adding diethylether after dissolving in acetone resulted in a pure complex which was vacuum filtered and dried. For the Ir–Pt dinuclear complex **(22)**, the mononuclear complex **(20)** was reacted with $[Pt(dmso)_2Cl_2]$ in DCM. The complex precipitated from solution and was vacuum filtered, dissolved in acetone and reprecipitated by adding hexane and diethylether. For the homodinuclear Ir–Ir complex **(23)**, rather than taking two equivalents of the bridging ligand, a 1:1 mixture of the dichlorobridged precursor and bpm ligand was reacted in a DCM/MeOH (2:1) mixture, and heated at reflux temperature for 7 h, after which solvents were removed and the residue was dissolved in water which was filtered to remove any excess bpm ligand. A saturated aqueous KPF_6 solution was added to the filtrate, resulting in precipitation of the PF_6 complex which was then recrystallised from acetone/water (2:1) and dried. The synthesis of the mononuclear iridium complex with the ligand dpp is exactly the same as that explained above for the other

mononuclear complexes. Sufficient care has to be taken while adding the dichlorobridged iridium precursor complex slowly drop by drop in a 4-h time interval. After the reaction, solvents were removed, dissolved in water and filtered to remove any excess amount of dpp and the complex was precipitated by counter ion exchange by adding saturated aqueous KPF_6. The product was recrystallised from acetone/water and dried.

2.6 Photocatalytic H_2 Production Experiments

Luminescent iridium (III) transition metal complexes are very appealing because of the synthetic modifications possible for the ligands, which allow manipulation of the photophysical and electrochemical properties of these complexes for various applications, including photocatalysis (Hosono and Kaneko, 1997; Esswein and Nocera, 2007; Rau et al., 2007). An examination of the various iridium photocatalysts reported now is given in Section 2.1. Most of the cyclometallated iridium complexes prepared in this project showed good photocatalytic activity. In this section, the difference in photocatalytic properties between the iridium complexes as a function of the bridging ligands, bpp, tpy and bpm, is described. In some cases, experiments were carried out at four different water percentages (0%, 5%, 10% and 15%), of which the 5% composition was found to be the most effective for hydrogen production. The effect of ester groups on the photocatalytic activity was also considered. All the measurements were carried out at two different excitation wavelengths, UV light (350 nm) and visible light (470 nm). Intramolecular photocatalysis was carried out using the novel Ir–Pt/Pd systems which are the first of their kind of heterodinuclear iridium complexes. Intermolecular experiments were carried out for all the mononuclear iridium complexes using two different catalysts ($[Pt(ACN)_2Cl_2]$ and $[Pd(ACN)_2Cl_2]$). In all the photocatalytic experiments carried out, TEA was used as the sacrificial agent, ACN was used as the solvent and water as the proton donor.

2.7 Intermolecular Photocatalysis of $[Ir(ppy)_2(N^N)]PF_6$ Complexes

The strong reducing strength of the excited state of iridium cyclometallated complexes enables effective catalysis of the reduction of water to hydrogen. The $[Ir(ppy)_2(bpy)]PF_6$ complex and various analogues having substituents on both the ppy and bpy ligands have been studied by Bernhard and co-workers in the past few years (Slinker et al., 2004; Goldsmith et al., 2005; Lowry et al., 2005; Singh Bindra, 2012). In the present study, photocatalysis was investigated for the above-mentioned complexes by making changes to the structure of the photosensitiser and varying the conditions, which include:

- Investigating the impact of synthetic modification on photosensitiser performance as a result of deuteriation of the N^N ligand;
- Using two different platinum and palladium catalysts, $[Pt(ACN)_2Cl_2]$ and $[Pd(ACN)_2Cl_2]$, respectively, rather than the conventional K_2PtCl_4 and potassium tetrachloropallidate (K_2PdCl_4) salts; and
- By photocatalytic irradiation using two different wavelengths of light – visible light (470 nm) and UV light (350 nm).

Figure 2.5 presents an overview of the amount of hydrogen formed as expressed in TONs for complexes **(1)**–**(8)**, following irradiation under both visible light (470 nm) and UV light (350 nm). A set of eight complexes with the cyclometallated ppy ligand was prepared, having protonated and deuteriated N^N ligands. A number of observations can be made concerning these results. Firstly, that the TONs obtained are lower than those obtained by Lowry et al. (2005). The reasons for this are at present not clear. Secondly, the effect of deuteriation of the ligands is unexpected. When the compounds are irradiated at 450 nm the non-deuteriated compounds show higher TON values, while upon irradiation at 350 nm the reverse is observed. Further experiments are needed to understand these observations.

The tabulated TON values for intermolecular photocatalysis with $[Pt(ACN)_2Cl_2]$, along with the areas obtained using gas chromatographic measurement for

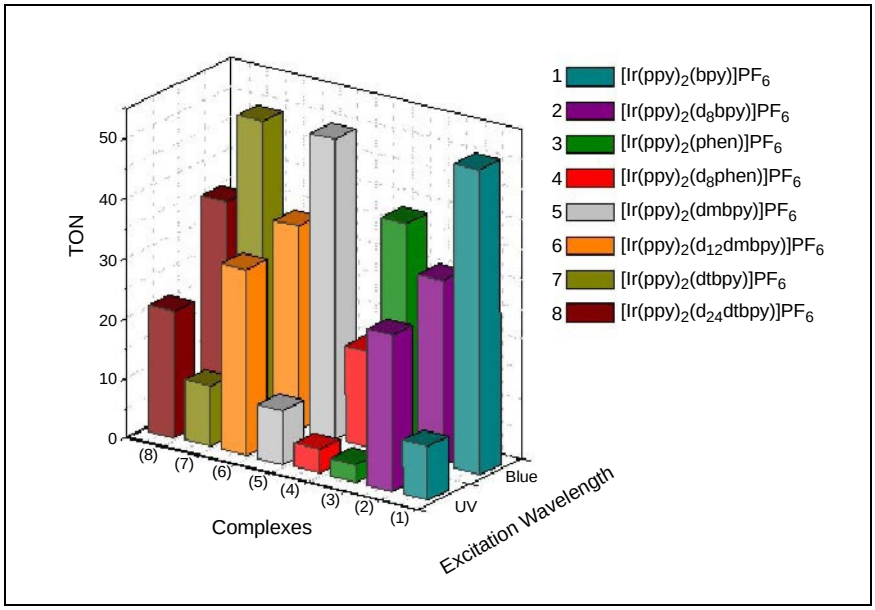

Figure 2.5. Schematic representation of the photocatalytic turnover number (TON) values for complexes (1) to (8) obtained in acetonitrile for both visible (470 nm) and UV (350 nm) light irradiation. Irradiation time 18 h, sacrificial reagent used triethylamine, concentration of photosensitiser and platinum catalyst 6 × 10^{-5} M.

both visible (470 nm) and UV (350 nm) light, are given in Table 2.1. Previous reports of photocatalysis using conventional platinum and palladium salts ($K_2[PtCl_4]$ and $K_2[PdCl_4]$) (Esswein and Nocera, 2007; Rau et al., 2007) showed palladium catalysts to be more efficient than platinum catalysts. Interestingly, when $[Pt(ACN)_2Cl_2]$ and $[Pd(ACN)_2Cl_2]$ complexes were used as catalysts, only platinum led to the production of hydrogen. The data presented show that the nature of the catalyst plays a crucial role in determining the efficiency of the photocatalysis. It has been reported by Krishnan and Sutin (1981), Krishnan et al. (1985), Goldsmith et al. (2005), Fihri et al. (2008b) and Andreiadis et al. (2011) that molecular platinum and palladium species are reduced to form a colloidal catalyst under similar conditions to those applied in the present study. However, after 18 h of photolysis no precipitate was observed for platinum but when palladium was used as the catalyst there was some precipitation. This suggests aggregation of the palladium colloids at an earlier stage of photocatalysis, resulting in the decomposition of the palladium catalyst and a decrease in the catalytic activity. Confirmation of this can only be made by carrying out scanning electron microscopy (SEM) or transmission electron microscopy (TEM) measurements.

2.8 Intramolecular and Intermolecular Photocatalysis of Ir Complexes with the bpp Ligand

Photocatalysis of the six novel cyclometallated iridium complexes ($[Ir(ppy)_2(bpp)](PF_6)$ **(9)**, $[Ir(ppy)_2(bpp)PtCl]_2(PF_6)_2$ **(10)**, $[Ir(ppy)_2(bpp)PdCl]_2(PF_6)_2$ **(11)**, $[Ir(ppy\text{-}COOCH_3)_2(bpp)](PF_6)$ **(12)**, $[Ir(ppy\text{-}COOCH_3)_2(bpp)PtCl]_2(PF_6)_2$ **(13)** and $[Ir(ppy\text{-}COOCH_3)_2(bpp)PdCl]_2(PF_6)_2$ **(14)**) is discussed in this section.

2.8.1 Intramolecular photocatalysis using visible light (470 nm)

Many challenges exist in designing a complete homogeneous water-splitting system. Once compatible PS and water reduction catalyst (WRC) components are found, the electron transfer processes must be perfected for optimal performance. The catalyst systems must efficiently quench the photoexcited PS complex, and a long lifetime for the charge separated state is required. The natural photosynthetic machinery fulfils these requirements by precise control of spatial organisation, electronic coupling, and relative redox energies of the adjacent components, giving the systems directional charge transfer character. To accomplish these requirements

Table 2.1. Tabulated turnover number (TON) values with their respective areas obtained from gas chromatography for complexes (1) to (8).

Complex (6×10^{-5} M) + $Pt(ACN)_2Cl_2$ (6×10^{-5} M)	H_2O%	470 nm		350 nm	
		Area (mV/s)	TON (average)	Area (mV/s)	TON (average)
$[Ir(ppy)_2(bpy)](PF_6)$ (1)	5%	1) 88 2) 91 3) 85	51	1) 15 2) 17	9
$[Ir(ppy)_2(d_8bpy)](PF_6)$ (2)	5%	1) 58 2) 50 3) 52	31	1) 47 2) 45	26
$[Ir(ppy)_2(phen)](PF_6)$ (3)	5%	1) 70 2) 66 3) 66	39	1) 5 2) 7	3
$[Ir(ppy)_2(d_8phen)](PF_6)$ (4)	5%	1) 30 2) 25 3) 26	16	1) 7 2) 8	4
$[Ir(ppy)_2(dmbpy)](PF_6)$ (5)	5%	1) 86 2) 88 3) 85	50	1) 14 2) 16	9
$[Ir(ppy)_2(d_{12}dmbpy)](PF_6)$ (6)	5%	1) 57 2) 60 3) 62	34	1) 54 2) 55	31
$[Ir(ppy)_2(dtbpy)](PF_6)$ (7)	5%	1) 89 2) 84 3) 88	50	1) 16 2) 17	10
$[Ir(ppy)_2(d_{24}dtbpy)](PF_6)$ (8)	5%	1) 61 2) 59 3) 61	35	1) 37 2) 35	21

in the laboratory, the components can be linked using multidentate bridging ligands that orchestrate electron transfer by providing optimal spatial separation and electronic coupling. A series of ruthenium intramolecular systems in which a ruthenium light-absorbing unit is attached to different catalytic metals, such as platinum, palladium, cobalt, rhodium and manganese, has been studied, and these systems showed good catalytic efficiency for hydrogen production. In the case of iridium complexes, most photocatalysis reported was intermolecular using mononuclear complexes. The only intramolecular photocatalysts reported to date are by Dietzek et al. (2006), based on an Ir–Co system, and Chiorboli et al. (2003) used an Ir–Co self-assembly system. This shows the importance of the four novel Ir–Pt/Pd complexes discussed here.

The results obtained following 18 h irradiation, using visible light for the four novel heterobimetallic Ir–Pt/Pd complexes, $[Ir(ppy)_2(bpp)PtCl]_2(PF_6)_2$ **(10)**, $[Ir(ppy)_2(bpp)PdCl]_2(PF_6)_2$ **(11)**, $[Ir(ppy\text{-}COOCH_3)_2(bpp)PtCl]_2(PF_6)_2$ **(13)** and $[Ir(ppy\text{-}COOCH_3)_2(bpp)PdCl]_2(PF_6)_2$ **(14)**, are given in Fig. 2.6, which gives a three-dimensional plot of TON at four different percentages of water.

Photocatalysis was carried out using four different water percentages (0%, 5%, 10% and 15%). For both non-ester complexes **(10)** and **(11)**, the maximum yield of hydrogen was obtained with 5% water. At greater percentages of water, the TON for hydrogen decreased slowly. Both complexes showed photocatalytic activity at 0% water, as shown in Fig. 2.6 (there is the possibility that hydrogen may be formed by the decomposition of TEA). On comparing the two non-ester complexes $[Ir(ppy)_2(bpp)PtCl]_2(PF_6)_2$ **(10)** and $[Ir(ppy)_2(bpp)PdCl]_2(PF_6)_2$ **(11)**, the Ir–Pt complex **(10)** proved to be more efficient than the Ir–Pd complex **(11)**. A possible explanation for this behaviour is based

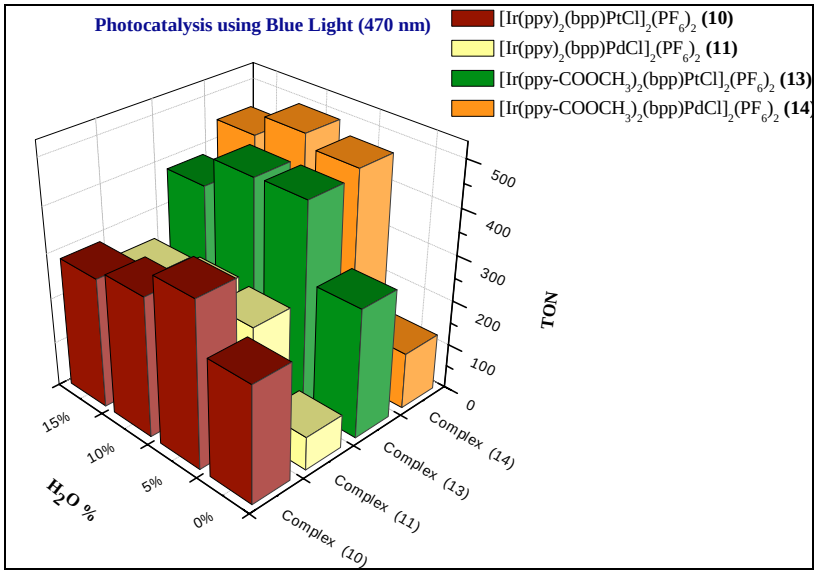

Figure 2.6. Three-dimensional representation of the photocatalytic turnover number (TON) values for hydrogen production for complexes (10), (11), (13) and (14) in acetonitrile using visible light (470 nm) irradiation. Irradiation time 18 h, sacrificial reagent used triethylamine, concentration of photosensitiser and catalyst 6×10^{-5} M.

on the photophysical properties. Compared with the mononuclear complex $[Ir(ppy)_2(bpp)](PF_6)$ **(9)**, the energy of the low-lying excited states is increased for both Ir–Pt **(10)** and Ir–Pd **(11)** complexes due to complexation of the iridium monomer with Pt/Pd. In the case of the platinum complex **(10)**, the energy of the $^3MLCT_{ppy}$ state increased by 0.26 eV, whereas there was only a slight increase of 0.01 eV for the palladium complex **(11)**. The net effect is that for the Ir–Pt complex the $^3MLCT_{ppy}$ excited state is increased in energy and populates the platinum-excited state at room temperature, resulting in more efficient photocatalysis. Such an increase in the energy of the excited state was not seen for the Ir–Pd complex **(11)**, which might be the reason for the decrease in catalytic efficiency compared with the Ir–Pt system.

The analogous ester complexes $[Ir(ppy\text{-}COOCH_3)_2(bpp)PtCl]_2(PF_6)_2$ **(13)** and $[Ir(ppy\text{-}COOCH_3)_2(bpp)PdCl]_2(PF_6)_2$ **(14)** showed significantly higher catalytic activity compared with the non-ester analogous complex. The ester platinum complex **(13)** showed maximum catalytic activity in solutions containing 5% and 10% water. At higher percentages of water, catalytic activity decreased. The ester palladium complex **(14)** showed maximum catalytic activity at 10% water. The ester complexes are much more efficient than the non-ester complexes for hydrogen formation. A possible explanation for this behaviour can be attributed to the photophysics for these complexes. Substitution of the peripheral phenyl pyridine ligand by ester groups resulted in an increase in the energy of the low-lying excited states as demonstrated in the emission spectra. For the ester platinum complex **(13)**, there was an increase of 0.12 eV in the energy of the lowest excited state compared with the non-ester complex **(10)**. For the ester palladium complex **(14)**, there was an increase of 0.13 eV in the energy of the lowest excited state compared with the non-ester complex **(11)**. This increase in energy more effectively promotes electron transfer to the platinum or palladium centre, thus increasing the catalytic activity. The palladium ester complex, Ir–Pd complex **(14)** shows greater catalytic activity than the Ir–Pt complex **(13)**, and the non-ester Ir–Pt complex **(10)** was more photocatalytically efficient than the Ir–Pd complex **(11)**. From the emission energies, the two ester complexes showed almost the same energy as is evident in the emission spectra (not shown). When emission spectra for complexes **(9)**–**(14)** are compared, the Ir–Pd complex **(14)** showed more quenching, which suggests that electrons reach the

palladium centre more efficiently, resulting in a higher TON value.

2.8.2 Intramolecular photocatalysis using UV light (350 nm)

Intramolecular photocatalysis for the above-mentioned four novel Ir–Pt/Pd complexes was also carried out using UV light (350 nm). All compounds have greater extinction coefficients at 350 nm than at 470 nm. The amount of hydrogen produced was considerably less (in some cases no hydrogen is produced) using this irradiation wavelength. A three-dimensional representation of the results for the four complexes, with four different percentages of water are given in Fig. 2.7.

Figure 2.7 clearly shows a decrease in TON on moving to 350 nm from 470 nm irradiation for all complexes. Only complex **(13)** produced hydrogen at 0% water. Complexes **(10)** and **(11)** produced small amounts of hydrogen at 10% water which is almost one-fifth of what was obtained under similar conditions using visible light. Similarly to the studies carried out using visible light, the Ir–Pt complex **(10)** was more efficient than the Ir–Pd complex **(11)**. The ester complexes **(13)** and **(14)** show maximum efficiency at 5% water and at higher concentrations of water TON values decreased. Similarly to the behaviour observed using visible light, UV irradiation leads to greater catalytic activity for the ester Ir–Pd complex **(14)**. Visible light (470 nm) is far more efficient than the UV light (350 nm) and a possible explanation for this can be given on the basis of the excited state measurements. From the excited state studies carried out with these complexes, a low-lying $^3MLCT_{ppy}$ state is thought to be responsible for populating the platinum and palladium excited states. For the ester complexes, substitution of the peripheral ppy ligand by the electron-withdrawing ester groups results in an increase in energy of the $^3MLCT_{ppy}$ excited state, as is evident by analysing the emission spectra of the non-ester and ester complexes.

2.8.3 Intermolecular photocatalysis using visible (470 nm) and UV (350 nm) light

Intermolecular photocatalysis was carried out with the mononuclear complex $[Ir(ppy)_2(bpp)](PF_6)$ **(9)**, using both visible (470 nm) and UV light (350 nm), with two different percentages of water (5% and 10%) in the presence of $[Pt(ACN)_2Cl_2]$ and $[Pd(ACN)_2Cl_2]$. The results obtained are shown in Fig. 2.8. The TONs are slightly higher for the solutions containing 5% water than for those containing 10% water. Visible light (470 nm) produced more hydrogen than UV light (350 nm), which is in agreement with the intramolecular photocatalysis.

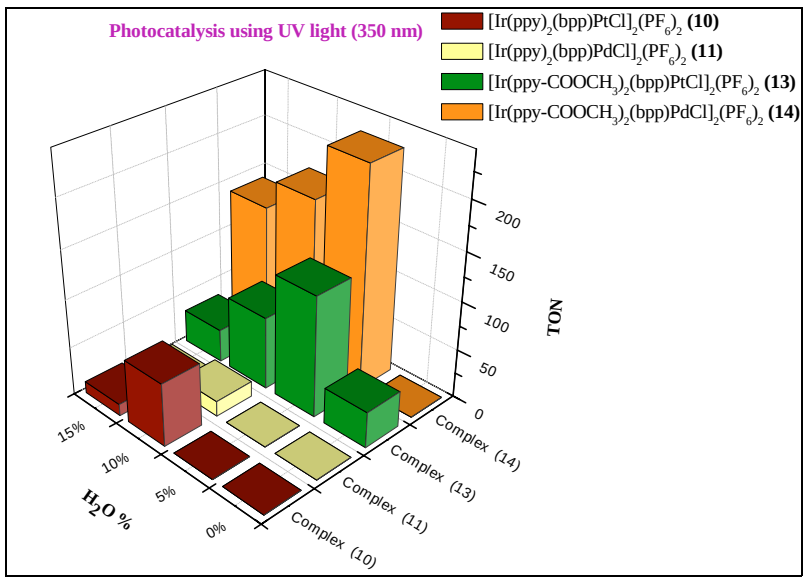

Figure 2.7. Three-dimensional representation of the photocatalytic turnover number (TON) values for complexes (10), (11), (13) and (14) in acetonitrile using UV light (350 nm) irradiation. Irradiation time 18 h, sacrificial reagent used triethylamine, concentration of photosensitiser and catalyst 6×10^{-5} M.

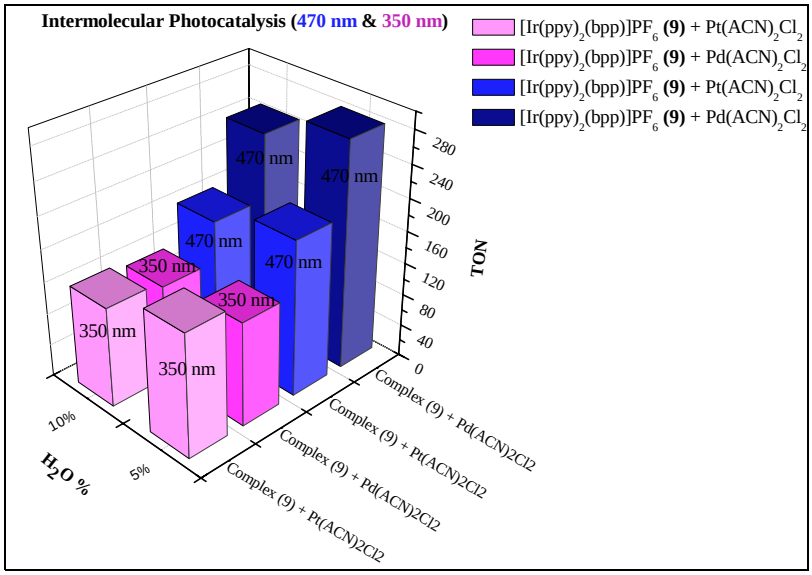

Figure 2.8. Three-dimensional representation of intermolecular photocatalytic turnover number (TON) values for complex (9) in acetonitrile using visible (470 nm) and UV (350 nm) light. Irradiation time 18 h, sacrificial reagent used triethylamine, concentration of photosensitiser and catalyst 6 × 10^{-5} M.

When the TONs for hydrogen production for complex **(9)** (Fig. 2.8) are compared with the two dimer complexes **(10)** and **(11)** using visible light, intramolecular photocatalysis is more efficient than intermolecular photocatalysis. However, when UV light is used intermolecular photocatalysis is more efficient than intramolecular photocatalysis. The photophysical data may provide an explanation. In the case of intramolecular photocatalysis, low-lying ^{3}MLCT states are populated and from here the excited state of platinum or palladium is populated at room temperature, when the system is in thermal equilibrium. From the absorption spectra, it is quite clear that these ^{3}MLCT excited states show absorption bands in the 400- to 500-nm range. Thus, excitation of these systems using the 470-nm results in direct population of the ^{3}MLCT levels from where an electron easily moves to Pt/Pd. However, when the wavelength is changed to 350 nm, the higher energy LLCT excited states are populated which, for the heterobimetallic Ir–Pt/Pd complexes, are much higher in energy than the platinum and palladium excited states, hence direct population of Pt/Pd excited states from this state is not as efficient as from the ^{3}MLCT states. This might be one possible explanation as to why intramolecular photocatalysis is more efficient using visible than UV light.

For the intermolecular systems studied here, one possible electron transfer mechanism may be as follows: after excitation the electron moves from the ground state to singlet ligand centred excited states, from where it decays to the triplet ligand-to-ligand excited state. For intermolecular photocatalysis, this ^{3}LLCT state plays the major role in populating the platinum and palladium centres. This assumption was made on the basis that intermolecular photocatalysis irradiation with 350 nm led to the formation of more hydrogen than did the intramolecular experiments. For these types of cyclometallated complexes, the ^{3}LLCT absorption band is reported to occur at around 350 nm (Polson et al., 2004). Further detailed studies are required to fully explain the differences observed. Based on the results presented here, these complexes may undergo photocatalysis through a reductive quenching mechanism as shown below:

$$PS + hv \rightarrow PS^* \quad (1)$$

$$PS^* + SR \rightarrow PS^- + SR^+ \quad (2)$$

$$PS^- + H^+ \rightarrow PS + \tfrac{1}{2}H_2 \quad (3)$$

Interestingly, the analogous non-ester ruthenium complexes containing the bpp ligand, which was synthesised within the group, gave lower amounts of hydrogen than the iridium counterparts.

2.8.4 Time-dependent intramolecular and intermolecular photocatalysis using visible light

Time-dependent intramolecular photocatalysis using visible light (470 nm) was carried out using $[Ir(ppy)_2(bpp)PtCl]_2(PF_6)_2$ **(10)** and $[Ir(ppy)_2(bpp)PdCl]_2(PF_6)_2$ **(11)**. Photocatalysis was performed in ACN, using TEA as the sacrificial agent. The graphical representation of the TONs obtained every hour for a period of 8 h is given in Fig. 2.9. This figure indicates that the Ir–Pt complex **(10)** showed greater catalytic activity than the Ir–Pd complex **(11)**. The Ir–Pt complex **(10)** gave a TON value of 630 after 7 h, and then began to decrease. After 18 h irradiation the TON value obtained was 364. This decrease in the amount of hydrogen formed after 8 h may possibly be due to leakage, or decomposition of the catalyst. For the Ir–Pd complex **(11),** no hydrogen was produced up to 2 h, thereafter the amount of hydrogen produced increased consistently and reached a TON value of 245 after 8 h irradiation. After 18 h **(11)** a TON of 249 was observed. From these TON values, it appears that the amount of hydrogen produced remains constant after 8 h irradiation for the Ir–Pd complex.

Time-dependent intermolecular photocatalysis was carried out with $[Ir(ppy)_2(bpp)](PF_6)$ **(9)** under similar conditions, but using two different catalysts $[Pt(ACN)_2Cl_2]$ and $[Pd(ACN)_2Cl_2]$. The graphical representation of the TONs obtained every hour for a period of 8 h is given in Fig. 2.10. From the figure, it is quite clear that in both cases the amount of hydrogen produced increases constantly from 1 h to 8 h. Thus, the photocatalysis is efficient, as neither the PS nor the catalyst are decomposing over this time period.

It is clear that intramolecular is more efficient than intermolecular photocatalysis. Furthermore, for the intramolecular photocatalytic experiments, the Ir–Pt complex **(10)** showed better photocatalytic efficiency than the Ir–Pd complex **(11)**. In the case of the intermolecular photocatalytic experiments using $[Pt(ACN)_2Cl_2]$ and $[Pd(ACN)_2Cl_2]$, the reverse was observed.

2.9 Intramolecular and Intermolecular Photocatalysis of IR Complexes with the tpy Ligand Using Visible and UV Light

Photocatalysis of five novel cyclometallated iridium complexes containing the tpy ligand is discussed. The

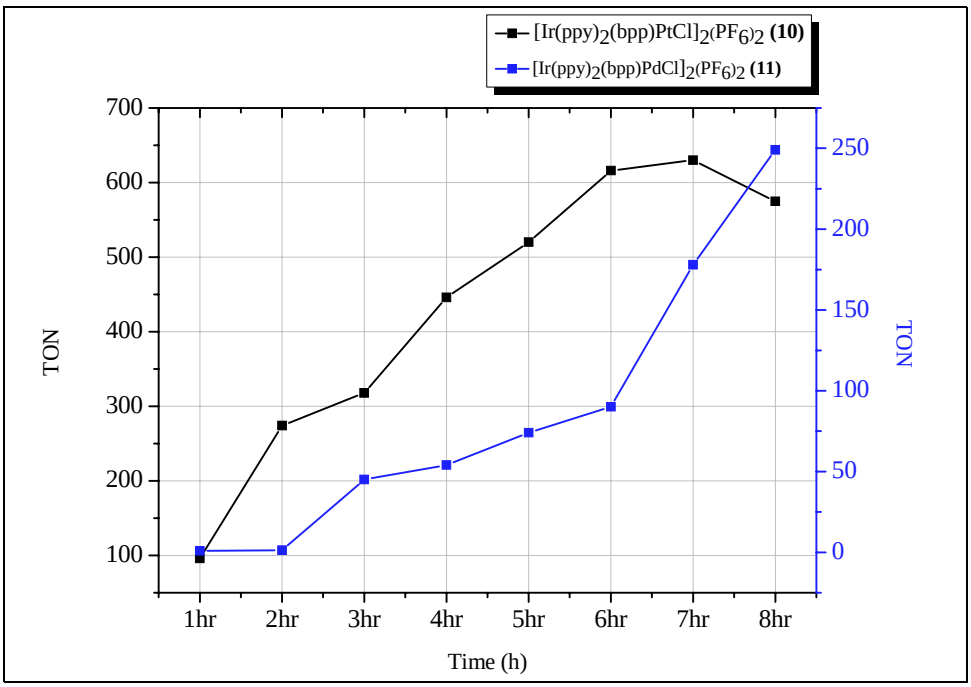

Figure 2.9. Graphical representation of time-dependent intramolecular photocatalysis using 470 nm visible light in 5% water/acetonitrile solution, the sacrificial reagent used is triethylamine.

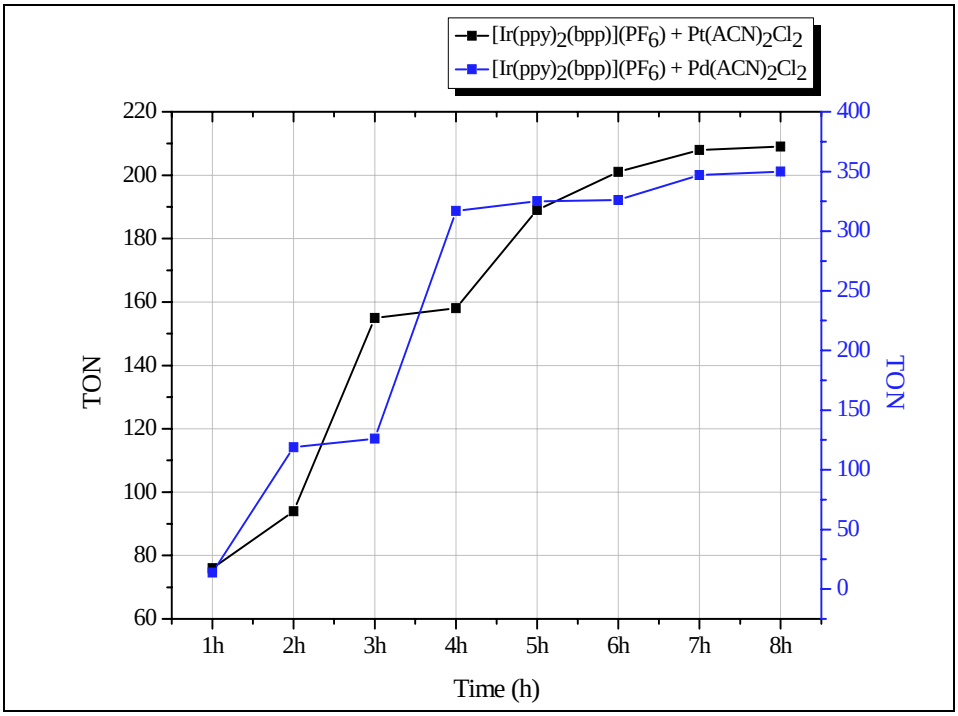

Figure 2.10. Graphical representation of time-dependent intramolecular photocatalysis using 470 nm (visible) light in a 5% water/acetonitrile solution, the sacrificial reagent used is triethylamine.

three mononuclear complexes are $[Ir(ppy)_2(tpy)](PF_6)$ **(15)**, $[Ir(ppy\text{-}COOCH_3)_2(tpy)](PF_6)$ **(17)** and $[Ir(ppy\text{-}CHO)_2(bpp)](PF_6)$ **(19)** and the two dinuclear Ir–Pd complexes are $[Ir(ppy)_2(tpy)PdCl]_2(PF_6)_2$ **(16)** and $[Ir(ppy\text{-}COOCH_3)_2(tpy)PdCl]_2(PF_6)_2$ **(18)**. Using TEA as the sacrificial agent, photocatalysis was carried out in ACN containing 5% water. The results following 18 h irradiation for both irradiation wavelengths are given in Fig. 2.11. It is interesting to note that neither of the heterobimetallic dinuclear Ir–Pd complexes $[Ir(ppy)_2(tpy)PdCl]_2(PF_6)_2$ **(16)** and $[Ir(ppy\text{-}COOCH_3)_2(tpy)PdCl]_2(PF_6)_2$ **(18)** produced hydrogen. The results obtained, however, for the intermolecular photocatalytic experiments using complexes **(15)**, **(17)** and **(19)** in conjunction with $[Pt(ACN)_2Cl_2]$ and $[Pd(ACN)_2Cl_2]$ gave varied results.

The unsubstituted ppy complex **(15)** formed hydrogen only in the presence of $[Pt(ACN)_2Cl_2]$ as the catalyst and no hydrogen when $[Pd(ACN)_2Cl_2]$ was used. UV irradiation produced marginally more hydrogen than the visible light. This is in contrast to the ester substituted complex **(17)**, which in the presence of $[Pt(ACN)_2Cl_2]$ gave almost the same amount of hydrogen for both visible and UV light irradiation. The use of $[Pd(ACN)_2Cl_2]$ as a catalyst resulted in a very large TON for **(17)** when visible light was used, but no hydrogen was produced using UV light. The analogous non-ester ruthenium mononuclear complexes with the tpy ligand produced no hydrogen in the intermolecular photocatalytic experiments, clearly indicating the higher efficiency of iridium metal photocatalysts. For the intramolecular systems, neither iridium nor ruthenium showed any hydrogen production activity (Singh Bindra, 2012).

2.10 Intramolecular and Intermolecular Photocatalysis of Ir Complexes Containing the bpm Ligand Using Both Visible and UV Light

Photocatalysis of three novel cyclometallated iridium complexes containing the bpm ligand is discussed in this section. The complexes include two mononuclear complexes $[Ir(ppy)_2(bpm)](PF_6)$ **(20)** and $[Ir(ppy\text{-}COOCH_3)_2(bpm)]$ (PF_6) **(24)** and one dinuclear Ir–Pd complex $[Ir(ppy)_2(bpm)PdCl_2](PF_6)$ **(21)**. The results obtained for both intermolecular and intramolecular photocatalysis using both visible (470 nm) and UV (350 nm) light in an ACN solution containing 5% water, TEA and either a palladium or platinum catalyst are

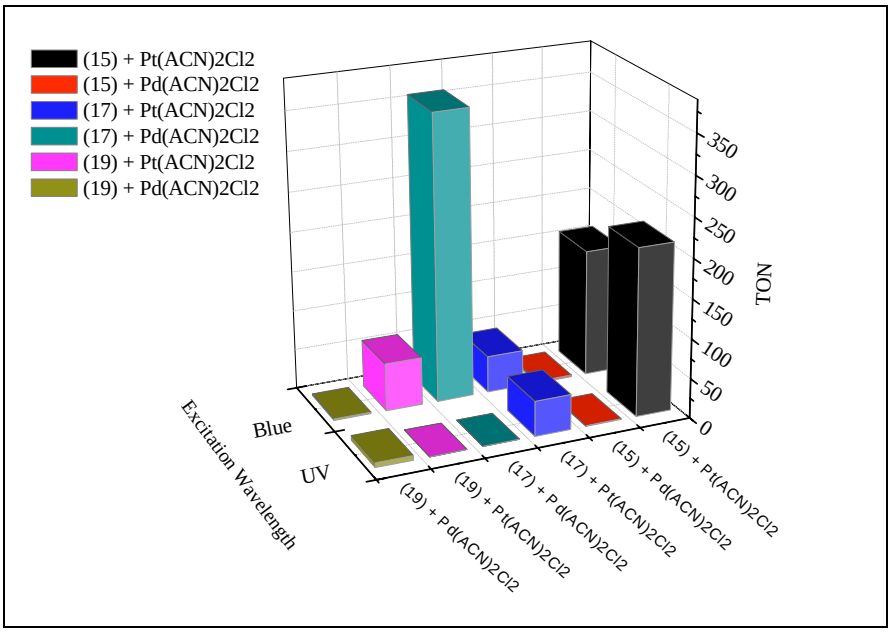

Figure 2.11. Three-dimensional representation of intermolecular photocatalytic turnover number (TON) values for complexes (15), (17) and (19) in acetonitrile using visible (470 nm) and UV (350 nm) light irradiation. Irradiation time 18 h, sacrificial reagent used triethylamine, concentration of photosensitiser and catalyst 6 × 10^{-5} M.

given in Table 2.2. The TON values obtained for these complexes are lower than those obtained for the iridium complexes discussed in the last section. Interestingly, the Ir–Pd dinuclear complex showed better photocatalytic activity than the intermolecular photocatalytic systems.

Table 2.2. Tabulated turnover number (TON) values for complexes (20), (21) and (24) in acetonitrile using visible light (470 nm) and UV light (350 nm). Irradiation time 18 h, sacrificial reagent used triethylamine, concentration of photosensitiser and catalyst is 6 × 10^{-5} M.

Complex (6 × 10^{-5} M)	**470 nm** TON_{H_2}	**350 nm** TON_{H_2}
$[Ir(ppy)_2(bpm)](PF_6)$ **(20)** + $Pt(ACN)_2Cl_2$	20	8
$[Ir(ppy)_2(bpm)](PF_6)$ **(20)** + $Pd(ACN)_2Cl_2$	3	2
$[Ir(ppy)_2(bpm)PdCl_2](PF_6)$ **(21)**	39	7
$[Ir(ppy\text{-}COOCH_3)_2(bpm)](PF_6)$ **(24)** + $Pt(ACN)_2Cl_2$	3	5
$[Ir(ppy\text{-}COOCH_3)_2(bpm)](PF_6)$ **(24)** + $Pd(ACN)_2Cl_2$	3	5

3 Organic Macrocycles Based on Porphyrins in Combination with a Bound Oxime Centre for the Production of Hydrogen

3.1 Introduction

Photocatalytic splitting of water was achieved by Zhu et al. (2011) using ethylenediaminetetraacetic acid (EDTA) as the sacrificial electron donor and a porphyrin-functionalised platinum colloid as the photocatalyst. TON_{Pt} and TON_{dye} were reported as 63 and 6,311, respectively, after irradiation with UV-Vis light for 12 h at a pH of 6.8. As the concentration of H^+ in the solution increases, the reduction of H^+ was found to occur at a faster rate. However, EDTA may be limiting as an electron source as its donating ability is decreased at low pH due to protonation. It was noted that no hydrogen TON was detectable from the complex when a visible light source was used due to the lack of strong absorbances in this region.

Intramolecular photo-induced hydrogen production has been reported by Hosono and Kaneko (1997) using viologen-linked porphyrins with EDTA as the sacrificial electron donor and a platinum hexachloride catalyst (H_2PtCl_6) as the catalytic centre (Fig. 3.1). The complexes were incorporated as $PtCl_6^{2-}$ ions and porphyrin cations into Langmuir–Blodgett (LB) films and irradiated with visible light ($720 > \lambda/nm < 390$) for 280 h.

The TONs of *p*-PC_5VC_{18} and *m*-PC_5VC_{18} were 5.2 and 16.8, respectively. The hydrogen evolution rate for *m*-PC_5VC_{18} was reported as almost three times greater than that of *p*-PC_5VC_{18}. It is proposed that this difference is due to configuration as the electron transfer rate and the redox potentials measured for

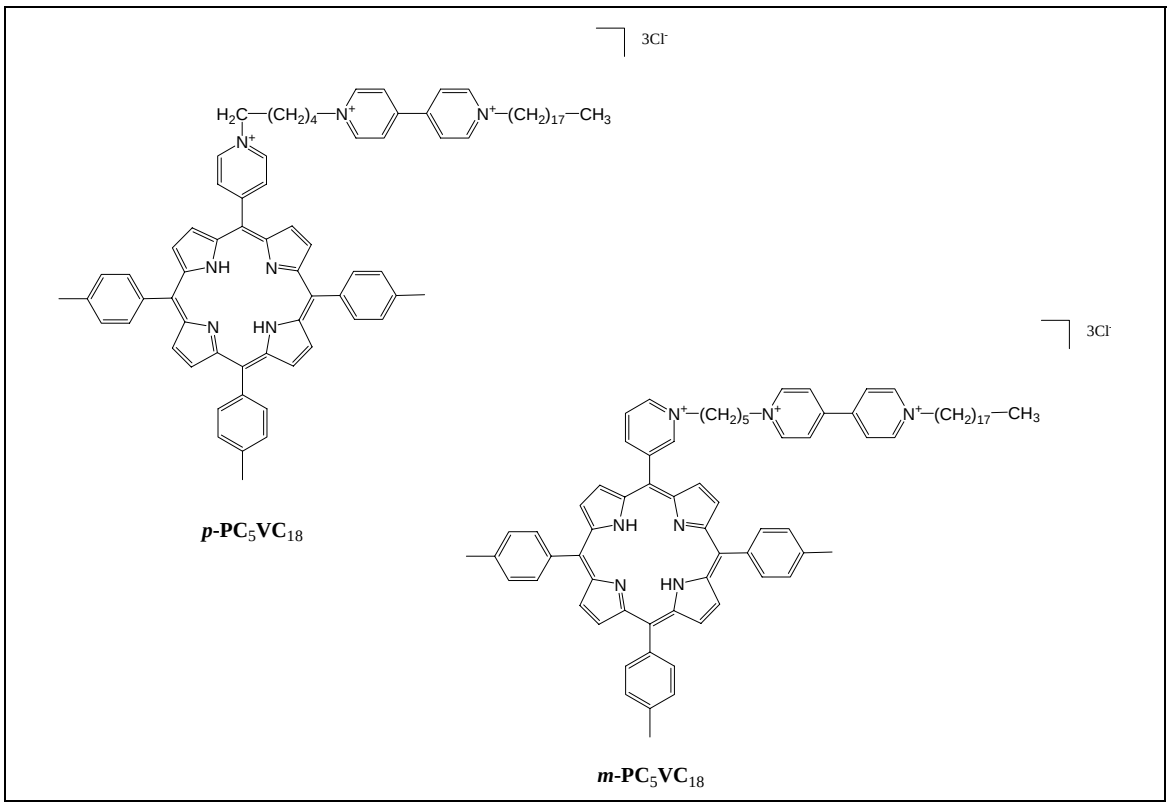

Figure 3.1. Viologen-linked porphyrins photosensitisers used by Hosono and Kaneko (1997).

both were almost identical. With regard to the shape of the *m*-PC_5VC_{18}, the functional groups in the molecule would be slightly more exposed to the water than those of *p*-PC_5VC_{18} and therefore more suitably configured for ease of interaction with the substrate.

While studying the efficacy of cobalt(II) tetraphenylporphyrin (CoTPP) and iron(II)-tetraphenylporphyrin (FeTPP) on the photoreduction of carbon dioxide to carbon monoxide, Dhanasekaran et al. (1999) report a competing side reaction, namely the generation of hydrogen. A carbon-dioxide-saturated solution of the complexes containing 5% TEA was irradiated at $\lambda > 300$ nm. It was found that CoTPP produced 1.6 mmol/l and FeTPP produced 3.4 mmol/l of hydrogen following 20 h irradiation. It was also found that the production of hydrogen continued using FeTPP even after the production of carbon monoxide had ceased.

More recently hydrogen production has been reported using a porphyrin photosensitiser and a cobaloxime catalytic centre. Zhang et al. (2010) have synthesised a monopyridyl triphenyl porphyrin co-ordinated to a cobaloxime chloride catalytic centre which has shown photo-induced hydrogen evolution using TEA as a sacrificial donor at 25°C using a 300 W Xe lamp with a cut-off filter, $\lambda_{exc} > 400$ nm. Using a solvent mixture of tetrahydrofuran/water (THF/H_2O) (8:2) yielded an optimum TON of 22 after 5 h for the zinc metallated porphyrin–oxime complex. The effect of the metallation of the porphyrin was demonstrated.

3.2 Synthesis of Porphyrin Macrocycles

Tetraphenylporphyrin (TPP), 5-pyridyl-15,20,25-triphenylporphyrin (MPyTPP) and their zinc-metallated complexes discussed in this chapter have been previously synthesised and all spectral data are in agreement with reported data. The cobaloxime derivatives are novel, and all spectral data are in agreement with their formulation and compare well with similar compounds that have been previously reported by Adler et al. (1967). All compounds were obtained in good yields ranging from 11% to 87%.

The ^{1}HNMR spectral signals of both MPyTPP and MPyTPP–cobaloxime due to the β-aromatic protons on the porphyrin ring system can be visible from 9.04 ppm to 8.65 ppm, with the protons closest to the pyridyl group being split into two sets of doublets at 9.04 ppm and 9.1 ppm. The addition of the cobaloxime moiety shifts all of the signals slightly upfield due to the shielding effect of the cobaloxime. The phenyl protons (2–4) appear in the aromatic region also. The signal from protons 2 appear more downfield than protons 3 and 4, which are on the outermost periphery of the porphyrin structure. Due to the presence of a lone pair on the nitrogen of the pyridyl group, protons 5 and 6 are observed at quite different ppm, with 6 appearing further upfield than proton 5. The two internal amine hydrogen (NH) protons (7) are observed at negative ppm values as there is a great amount of shielding due to the ring structure enclosing these protons, which generally appear at –2 ppm. The disappearance of these protons is used as an indication of successful metallation of the porphyrin ring. The co-ordination of the porphyrin to the cobaloxime moiety leads to the appearance of a strong singlet signal at 2.6 ppm (8); however, due to the nature of the constant exchange of proton 9* from glyoxime subunit to glyoxime subunit it is not always visible on ^{1}HNMR spectra and has not been reported in this study.

3.3 UV-Vis Spectroscopy

Room temperature absorption spectra were obtained for all compounds. All of the compounds in this study exhibit strong absorptions in the UV–visible region of the spectrum. Strong absorptions at ~416 nm, the Soret band, are assigned to ligand localised excitation into the second excited state, an S_0–S_2 (π–π^*) transition. The absorbance between 510 and 645 nm in each of the porphyrin complexes listed are generally attributed to S_0–S_1 (π–π^*) transition to the first, lowest energy excited state and are known as quasi-allowed (Q) bands. Due to the more symmetrical nature of metallated porphyrins, the number of these Q bands reduced from four to two following addition of a metal to the centre of the porphyrin ring.

3.4 Fluorescence Studies

Room temperature emission spectra were obtained for all compounds. Excitation into the Soret band of each of the porphyrin complexes gave rise to two emission bands with Stokes shifts between 7,290 cm^{-1} and 9,879 cm^{-1}. All of the zinc-metallated porphyrins gave

rise to a smaller Stokes shift than their freebase counterparts. The addition of a cobaloxime moiety had little to no influence on the emission profile, or the Stokes shift observed for the porphyrin complexes.

3.5 Photocatalytic H_2 Generation Studies

Experiments to test for the photocatalytic generation of hydrogen from water were carried out in triplicate. The solutions were photolysed for 20 h using a blue light (470 nm) or a UV light (350 nm) LED light array. After 20 h, a 0.5-ml sample of the headspace in the reaction vial was collected using a gas-tight syringe. These samples were injected into a series CP-3800 gas chromatograph (GC) with both thermal conductivity and flame-ionisation detectors (TCD and FID) used in conjunction with one another. Unfortunately, the amount of hydrogen produced was low, and the authors were unable to quantify it.

3.6 Photoelectrocatalytic H_2 Generation Studies

The compounds were also investigated using photoelectrocatalytic techniques. They were immobilised on electrode surfaces using the drop-casting technique. Each modified electrode was tested using an applied potential of –1.2 V for 1 h and the resulting hydrogen TONs generated were compared. A 1-ml sample of the headspace was injected into a GC and the GC-calculated TONs were compared with those calculated electrochemically to measure the overall efficiency of the electrochemical reaction (Table 3.1).

It is evident from the results presented in Table 3.1 that the TONS generated with these three complexes were consistent with the observed intensity of the catalytic current induced. The current density measured over the course of the hour-long bulk electrolysis experiment at –1.2 V was found to be 2.759 mA/cm^2, producing an electrochemically determined TON of 10,384 when using MPyTPP, while the current density measured when using MPyTPP–obaloxime was significantly less at 1.07 mA/cm^2, yielding a TON of 3,680, implying a higher catalytic activity utilising the porphyrin alone. TPP produced the most enhanced catalytic current and also the largest electrocatalytically determined TON of 13,640 after 1 h. The efficiencies of the systems were calculated by injecting a portion of the headspace in the reaction vessel onto a GC and analysing it for its hydrogen content. This GC-generated TON is a more accurate measurement of the number of moles of hydrogen produced as it does not take background charging into account as the electrochemically generated TON does.

Table 3.1. Results of electrocatalytic studies for all porphyrin and porphyrin–cobaloxime complexes.

Compound	Charge passed after 1 h (C)	Electrochemical TON × 10^3	Gas chromatograph TON × 10^3	Efficiency %	Average current during bulk electrolysis (A) × 10^{-4}	Current density (mA/cm^2) × 10^{-3}
Cobaloxime	0.45	15.6	7.9	51	1.52	2.17
ZnMPyTPP	0.37	12.8	7.6	59	0.96	1.38
MPyTPP–Oxime	0.10	3.6	1.7	49	0.75	1.07
ZnMPyTPP–Oxime	0.22	7.8	5.1	65	0.80	1.14
ZnTPP	0.38	13.4	10.5	78	1.3	1.87

4 Ruthenium–Rhenium Complexes

4.1 Introduction

Recently, Ru(II)–Re(I) heterodinuclear complexes have been used for visible-light-driven conversion of carbon dioxide to products including carbon monoxide, formate or oxalate. Reduction of carbon dioxide to chemical energy can create a new green, pollution-free world as an alternative solution to the recent energy crisis and global warming. Ruthenium(II) carbonyl complexes (Oyama et al., 2003; Doherty et al., 2009) were extensively used as photocatalysts for the reduction of carbon dioxide. Ruthenium and cobalt polypyridyl metal complexes absorb light in the visible region and, therefore, can act as a photosensitiser as well as an active catalytic centre for the reduction of carbon dioxide. Carbon monoxide was found to be the principal reduced product of carbon dioxide in all the reported catalytic processes. Rhenium(I) carbonyl complexes have been studied by many research groups to understand and investigate the catalytic process involved in the photo-reduction of carbon dioxide. Rhenium(I) carbonyl complexes absorb light in the UV region (~365 nm), whereas Ru(II)–Re(I) heterodinuclear complexes absorb light at longer wavelengths, greater than 430 nm as reported by Stufkens and Vleck (1998), Riklin et al. (2001), Possamai et al. (2006) and Doherty et al. (2009). Therefore, Ru–Re heterodinuclear photocatalysts are more advantageous than the rhenium mononuclear carbonyl complexes in terms of visible-light-driven photocatalysis.

Currently, artificial photosynthesis is a vibrant research topic. Vogler and Kisslinger (1986), Sahai et al. (1989), Van Wallendael et al. (1990), Kalyanasundaram et al. (1992), Bardwell et al. (1995), Encinas et al. (2001), Takeda and Ishitani (2009) and Yamamoto et al. (2010) reported a wide range of mononuclear rhenium(I) and Ru(II)–Re(I) heterodinuclear complexes. Most recently, a rhenium complex, typically named rhenium(I) phenanthroline-polyoxometalate hybrid, reported by Ettedgui et al. (2011), was used as the active photocatalyst for the reduction of carbon dioxide. In all the cases, the ruthenium(II) moiety acted as a photosensitiser where the peripheral ligands at the ruthenium(II) centre were 2,2-bipyridine and 4,4'-dimethyl-2,2'-bipyridine. Rhenium(I) tricarbonylchloride acted as an active catalytic centre.

Bridging ligands play an important role in binding photosensitisers and the photocatalytic metal centre together to form a heterodinuclear photocatalyst. The bridging ligand is the mediator, which transfers the excited-state electrons to the catalytic centre. The bridging ligands utilised in this study are quite different from those previously reported by Ishitani and co-workers. Previously reported bridging ligands used by Ishitani's research group were made of two bipyridine units connected with an aliphatic chain. The Ru–Re heterodinuclear complexes containing non-conjugated bridging ligands were also successful in reducing carbon dioxide, with high TONs of more than 240. The main reason behind such high TONs is the correct energy level overlap between the bridging ligand and the catalytic rhenium centre. The bridging ligands used here are conjugated in nature. Therefore, it is anticipated that conjugation in the ligand will facilitate electron transfer from the ruthenium photosensitiser to the rhenium catalytic centre. Moreover, the conjugated bridging ligands should also meet the criteria of energy-level overlapping for the effective electron transfer. Photocatalysis using an Ru–Re heterodinuclear system was first introduced by Takeda et al. (2008), Takeda and Ishitani (2009) and Bian et al. (2009) who synthesised a series of Ru–Re heterodinuclear catalysts for carbon dioxide reduction. Here, the ultimate aim is to carry out heterogeneous catalysis on the surface of semiconductors using Ru–Re photocatalysts.

4.2 Synthesis and Isolation of Ru–Re Complexes

The Ru–Re heterodinuclear complexes synthesised and characterised in this project are examples of a number of Ru–Re heterodinuclear complexes containing carboxy ester groups. Carboxy groups are

known as good anchors for the semiconductors; therefore, Ru–Re heterodinuclear complexes can be bound to the surface of semiconductors. The bridging ligands used for synthesising Ru–Re heterodinuclear complexes are shown in Fig. 4.1. These ligands were initially isolated before attempting the synthesis of the complexes.

A number of rhenium(I) tricarbonyl mononuclear complexes were synthesised using toluene. Two new rhenium(I) tricarbonyl complexes were reported in this chapter which are based on carboxy and phosphonate functionalised bpy ligands. These complexes can also be bound to the semiconductor surface in order to carry out heterogeneous catalysis. The reaction for synthesising such rhenium mononuclear complexes is shown in Reaction 4.1.

The synthetic procedure involving methanol as a solvent, proposed by Van Wallendael et al. (1990), was modified and ethanol was employed as a solvent to synthesise Ru–Re heterodinuclear complexes containing carboxy ester (ethyl) groups. These carboxy ester groups are not stable at high temperature and can be hydrolysed; therefore, modification of the synthetic procedure was essential. Spectroscopic-grade ethanol was used as a reaction solvent instead of methanol so that there was no exchange of methyl and ethyl ester groups at high reflux temperatures. Furthermore, the ruthenium complex dissolves better in ethanol. The work-up procedure was also altered considering the carboxy ester groups. Column chromatography was not performed to purify these complexes since they stick to the column, hence lowering the overall yield. Therefore, two work-up procedures were applied to purify the products. The reaction for synthesising $[Ru(R_2bpy)_2(2,5\text{-}dpp)Re(CO)_3Cl]^{2+}$ complexes (R = H, $COOC_2H_5$) is shown in Reaction 4.2.

The same reaction procedure was further applied as a general reaction procedure for synthesising other Ru(II)–Re(I) heterodinuclear complexes. The synthesised Ru–Re heterodinuclear complexes are shown in Fig. 4.2.

Any excess of rheniumpentacarbonylchloride ($[Re(CO)_5Cl]$) in the crude product can be removed by

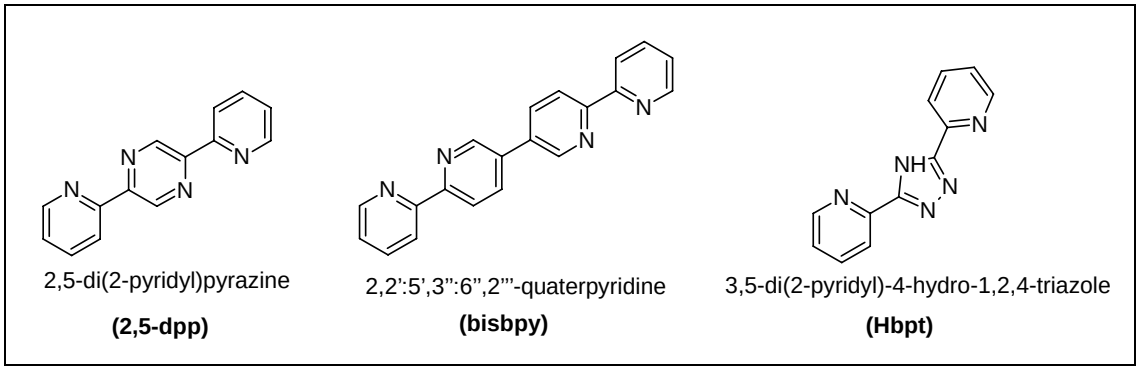

Figure 4.1. List of bridging ligands and their structures.

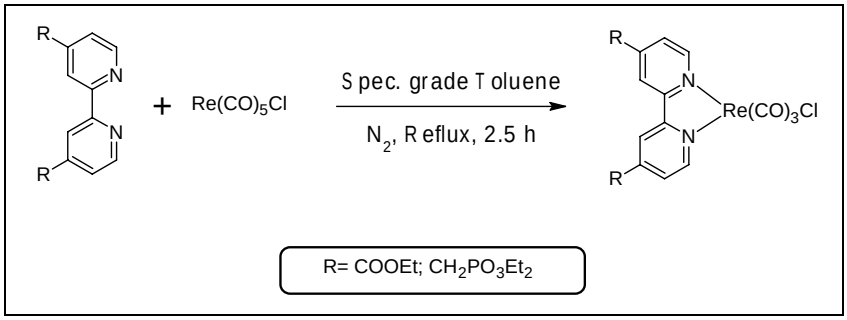

Reaction 4.1. Reaction for synthesising $[(L)Re(CO)_3Cl]$ complexes. L = dceb and dpb.

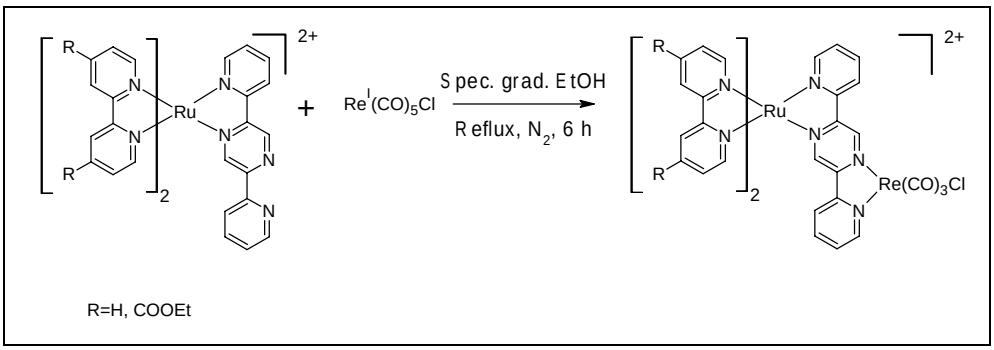

Reaction 4.2. The reaction for synthesising $[Ru(R_2bpy)_2(2,5\text{-}dpp)Re(CO)_3Cl]^{2+}$ (R = H, $COOC_2H_5$).

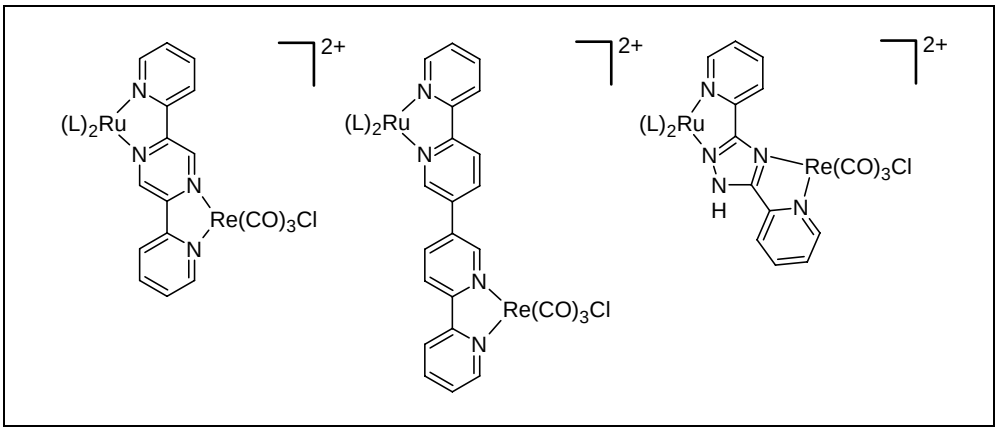

Figure 4.2. List of ruthenium(II)–rhenium(I) heterodimetallic complexes synthesised (L = 2,2'-bipyridine, d_8-2,2'-bipyridine, 4,4'-diethylcarboxy-2,2'-bipyridine).

washing with non-polar organic solvents, as the Ru–Re heterodinuclear complexes are not soluble in non-polar solvents such as hexane and pentane. The non-polar solvent was usually faint green in colour following washing and this is thought to be due to the formation during the reaction of a small amount of rhenium oxide (which is green in colour) which is a result of the decomposition of the Ru–Re heterodinuclear complex. The reaction colour turned from red to greenish red when the reaction was carried out for more than 6 h. It is recommended to carry out the reaction within 6 h to prevent the possible decomposition of the heterodinuclear complexes, leading to a lowering of the product yield.

Another way of removing rhenium oxide is by passing the reaction solution through a celite layer. But, there is a drawback in applying this procedure for the carboxy-derivatised complexes. Celite contains 80–90% silica and also other metals, such as sodium and potassium, which may result in the ester compounds undergoing hydrolysis and, further, they may then be adsorbed onto the celite particles. When Ru–Re heterodinuclear compounds were passed through a celite layer, they were absorbed onto the celite, turning it red in colour. It proved impossible to remove the complexes from the celite layer, even after washing with highly polar solvents such as acetonitrile.

Using the above optimised reactions and modified work-up procedures, a number of novel Ru–Re heterodinuclear and rhenium(I) mononuclear complexes were synthesised. The compounds were characterised by NMR, infrared, UV-Vis and emission spectroscopy.

4.3 Absorption and Emission Spectra of Mononuclear Complexes

An understanding of the absorption and emission spectra of mononuclear ruthenium and rhenium-

carbonyl complexes is essential before analysing the absorption and emission spectra of Ru–Re heterodinuclear complexes. For the absorption and emission properties of the ruthenium mononuclear complexes an increase in the MLCT band (>452 nm) was observed with the introduction of the electron-withdrawing carboxy ester groups compared with $[Ru(bpy)_3]^{2+}$. Past literature reports by Sahai et al. (1989), Yamamoto et al. (2008) and Ioachim et al. (2006) suggest that $[(bpy)Re(CO)_3Cl]$ has its lowest energy absorption band at 390 nm which is assigned to an MLCT transition. The low-energy absorption bands for the mononuclear rhenium complexes ($[(dceb)Re(CO)_3Cl]$ and $[(dpb)Re(CO)_3Cl]$) discussed in this report are assigned to MLCT transitions on comparing with $[(bpy)Re(CO)_3Cl]$. The absorption maximum of $[(dceb)Re(CO)_3Cl]$ is found at lower energy compared with that of $[(bpy)Re(CO)_3Cl]$. Kalyanasundaram and Nazeeruddin (1990) report that the dceb has a lower π^* level compared with the bpy ligand and therefore results in a lowering of the energy gap between the highest occupied molecular orbital (HOMO) and the lowest unoccupied molecular orbital (LUMO) for $[(dceb)Re(CO)_3Cl]$ compared with $[(bpy)Re(CO)_3Cl]$ (Fig. 4.3).

Emission spectra of $[(dceb)Re(CO)_3Cl]$ and $[(dpb)Re(CO)_3Cl]$ were recorded in acetonitrile at room temperature. The emission maximum of $[(dpb)Re(CO)_3Cl]$ (617 nm) was red-shifted relative to $[(bpy)Re(CO)_3Cl]$ (600 nm) and no emission was observed for $[(dceb)Re(CO)_3Cl]$ at room temperature (Fig. 4.4). According to Wrighton and Morse (1974), Hawecker et al. (1983a,b), Worl et al. (1991), Ziessel et al. (1997, 1998), Lam et al. (2002), Hayashi et al. (2003) and Chan et al. (2005), the emission states for the rhenium(I) complexes are defined as ^{3}MLCT emitters. Therefore, it can also be inferred that the ^{3}MLCT state for the rhenium complex $[(dpb)Re(CO)_3Cl]$ is responsible for the emission wavelength observed at 617 nm. The $[(dceb)Re(CO)_3Cl]$ does not emit at room temperature and substantially quenched emission intensity was observed, which indicates lowering the gap between HOMO and LUMO levels created by the electron-withdrawing effect of the carboxy ester groups (Van Wallendael et al., 1990).

4.4 Absorption and Emission Spectra of Ru(II)–Re(I) Heterodinuclear Complexes

A number of Ru–Re heterodimetallic complexes based on dpm and 1,4,5,8,9,12-hexaazatriphenylene (HAT)

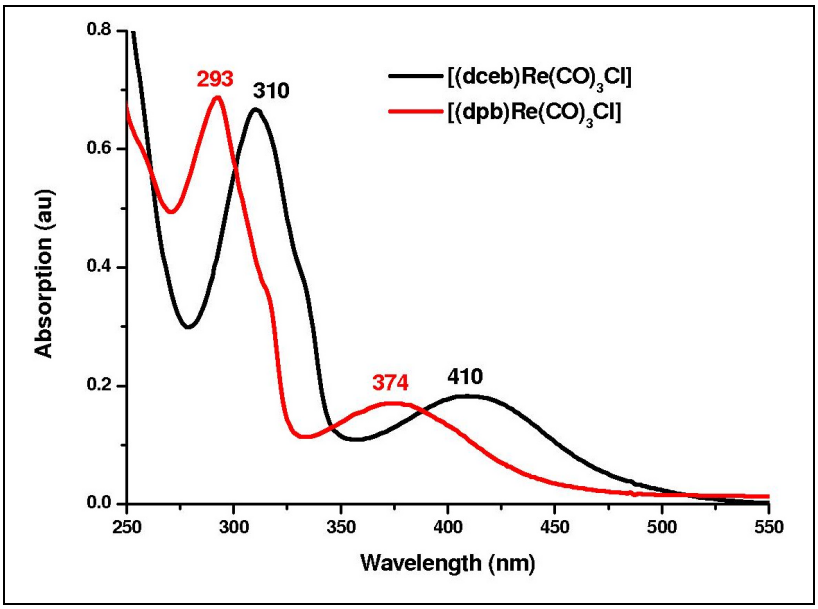

Figure 4.3. Absorption spectra of $[(dceb)Re(CO)_3Cl]$ (black) and of $[(dpb)Re(CO)_3Cl]$ (red). Absorption spectra of both compounds were recorded in acetonitrile at room temperature (20 ± 2°C).

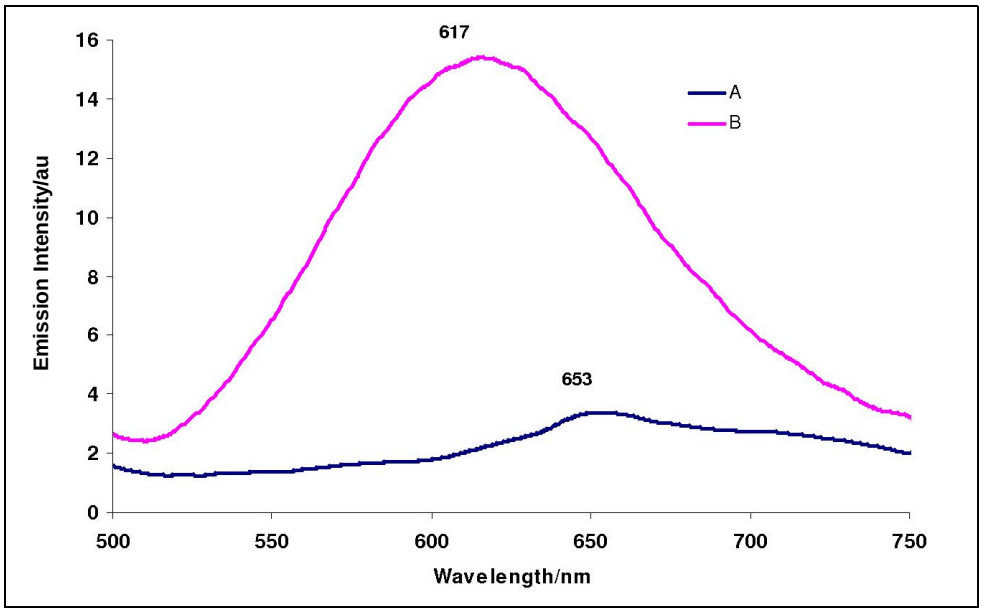

Figure 4.4. Emission spectra of [(dceb)Re(CO)$_3$Cl] (A) and [(dpb)Re(CO)$_3$Cl] (B). Emission spectra of both compounds were recorded in acetonitrile at room temperature (20 ± 2°C). OD at λ_{ex} = 0.2 au, λ_{ex} = 400 nm.

as bridging ligands were reported by Sahai et al. (1989). The higher and the lower energy transitions for Ru–Re heterodimetallic complexes were assigned to the rhenium metal to dpm or HAT-based MLCT transitions and the ruthenium metal to dpm or HAT ligand MLCT transitions, respectively. For example, [Ru(bpy)$_2$(dpm)Re(CO)$_3$Cl]$^{2+}$ has MLCT transitions at 558 nm and 414 nm, with a shoulder at 377 nm. The absorption band at 558 nm was assigned to a dπ(Re)–π^*(dpm)-based transition and that at 414 nm was assigned to a dπ(Re)–π^*(dpm)-based transition.

A red shift in the lowest MLCT band was observed in heterodinuclear complexes containing the bridging ligands with low-lying π^* levels, which indicates further lowering of the π^* levels of the bridge when attached to the Re(CO)$_3$Cl moiety (Constable and Seddon, 1982; Waterland et al., 1998; Rillema et al., 1990). For example, the mononuclear complex [Ru(bpy)$_2$(2,5-dpp)]$^{2+}$ has an absorption maximum at 433 nm, while the heterodinuclear complex [Ru(bpy)$_2$(2,5-dpp)Re(CO)$_3$Cl]$^{2+}$ has an absorption maximum at 552 nm. However, no shift in the MLCT bands was observed in the case of Ru–bisbpy–Re heterodinuclear complexes compared with the corresponding mononuclear Ru–bisbpy complexes. The mononuclear complex [Ru(bpy)$_2$(bisbpy)]$^{2+}$ and the heterodinuclear complex [Ru(bpy)$_2$(bisbpy)Re(CO)$_3$Cl]$^{2+}$ have an absorption maximum at 452 nm and 450 nm, respectively. Both the bpy units are twisted with respect to each other when the bisbpy ligand is bound to two metal centres (see Fig. 4.5). This hinders overlap between the π-orbitals on the two bpy units. As a result, the Ru(dπ)→bisbpy(π^*) MLCT is unaffected following complexation with the rhenium metal centre on the other side of the bisbpy ligand.

The absorption spectra for [Ru(bpy)$_2$(2,5-dpp)]$^{2+}$ and [Ru(bpy)$_2$(μ-2,5-dpp)Re(CO)Cl]$^{2+}$ are displayed in Fig. 4.6. It is important to mention that 2,5-dpp has a lower π^* level than the bpy ligands. According to Wrighton and Morse (1974), Hawecker et al. (1983a,b), Worl et al. (1991), Ziessel et al. (1997, 1998), Lam et al. (2002), Hayashi et al. (2003) and Chan et al. (2005), the lower energy of the MLCT band is dominated by a dπ(Ru)–π^*(2,5-dpp) transition for the mononuclear ruthenium complex. [Ru(bpy)$_2$(2,5-dpp)]$^{2+}$ has two MLCT bands, one at 433 nm and the other at 482 nm. The MLCT transition at 433 nm was assigned to dπ(Ru)–π^*(bpy) and at 482 nm to dπ(Ru)–π^*(2,5-dpp) transitions. It is also important to observe that the intraligand π–π^* transition for bpy and 2,5-dpp appears at ~290 nm and at 317 nm, respectively. Similarly, [Ru(bpy)$_2$(2,5-dpp)Re(CO)$_3$Cl]$^{2+}$ displays two π–π^* transitions for bpy and 2,5-dpp ligands. Interestingly, in the case of the Ru–Re heterodinuclear

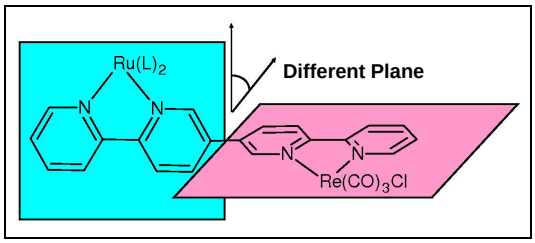

Figure 4.5. Two bpy units of bisbpy are in two different planes, which restrict the interaction between two metal centres in the rubidium–bisbpy–rhenium complex.

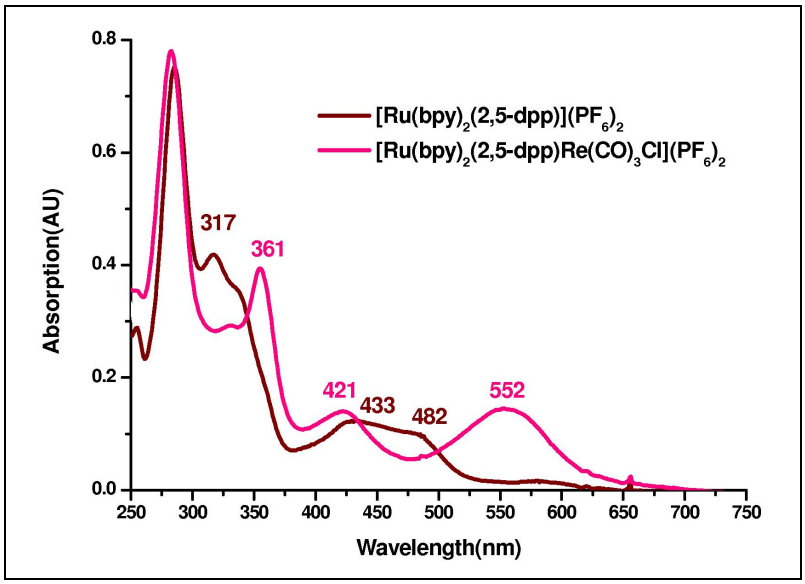

Figure 4.6. Absorption spectra of $[Ru(bpy)_2(2,5\text{-dpp})]^{2+}$ (brown) and of $[Ru(bpy)_2(\mu\text{-}2,5\text{-dpp})Re(CO)_3Cl]^{2+}$ (purple–red). Absorption spectra of both compounds were recorded in acetonitrile at room temperature (20 ± 2°C).

complex, a strong absorption band was observed at 361 nm. According to the literature, this is due to the introduction of a $Re(CO)_3Cl$ moiety, which lowers the π^* level of the 2,5-dpp ligand (Waterland et al., 1998). This results in further lowering of the energy gap between HOMO and LUMO levels in the heterodinuclear complex. The smaller energy gap between the HOMO and the LUMO itself suggests a lower energy absorption maximum. $[Ru(bpy)_2(2,5\text{-dpp})Re(CO)_3Cl]^{2+}$ has two MLCT bands, one at 552 nm and the other at 421 nm. According to the literature, the absorption band at 552 nm is assigned to a $d\pi(Ru)–\pi^*(2,5\text{-dpp})$ MLCT transition and the absorption band at 421 nm is assigned to a $d\pi(Re)–\pi^*(2,5\text{-dpp})$ MLCT transition. The $d\pi(Ru)–\pi^*(2,5\text{-dpp})$ MLCT transition for $[Ru(bpy)_2(2,5\text{-dpp})Re(CO)_3Cl]^{2+}$ is red-shifted from 482 nm to 552 nm compared with $[Ru(bpy)_2(2,5\text{-dpp})]^{2+}$.

An example of the emission spectra of heterodinuclear Ru–Re complexes is displayed in Fig. 4.7. $[Ru(bpy)_2(bisbpy)Re(CO)_3Cl](PF_6)_2$ shows an emission band at 661 nm whereas the corresponding ruthenium mononuclear complex $[Ru(bpy)_2(bisbpy)](PF_6)_2$ shows a band at 633 nm. The red shift in emission wavelength from 633 nm to 661 nm is due to the co-ordination of the $Re(CO)_3Cl$ moiety which stabilises the π^* level of bisbpy as reported by Rillema et al. (1990). On the other hand, the emission wavelength did not change

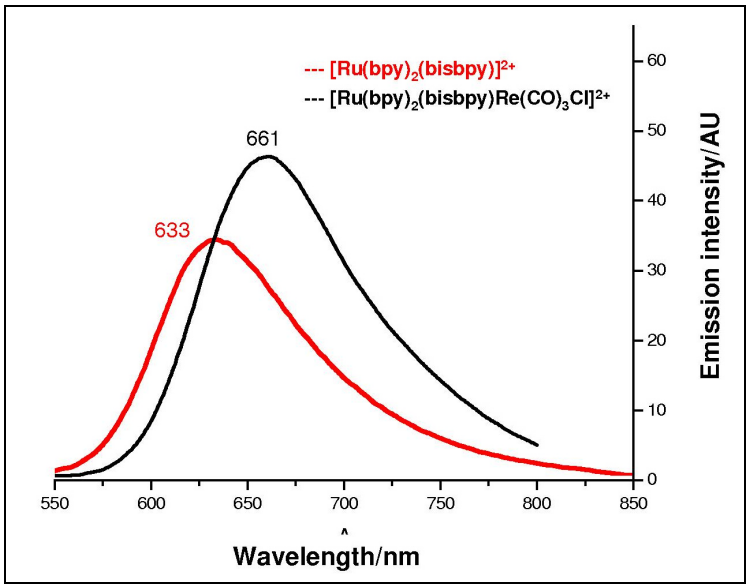

Figure 4.7. Emission spectra of $[Ru(bpy)_2(bisbpy)]^{2+}$ and $[Ru(bpy)_2(bisbpy)Re(CO)_3Cl]^{2+}$. Emission spectra of both compounds were recorded in acetonitrile at room temperature (20 ± 2°C). OD at λ_{ex} = 0.15 au, λ_{ex} = 450 nm.

for $[Ru(dceb)_2(bisbpy)Re(CO)_3Cl](PF_6)_2$ with the introduction of the $Re(CO)_3Cl$ moiety.

$[Ru(L)_2(\mu\text{-}2,5\text{-}dpp)Re(CO)Cl]^{2+}$ complexes (L = bpy and dceb) also have very weak or no emission at room temperature compared with mononuclear $[Ru(L)_2(2,5\text{-}dpp)]^{2+}$, which indicates an interaction between two metal centres. Also, the 2,5-dpp is a strong π- acceptor ligand and hence its π^* levels are stabilised by the co-ordination of the $Re(CO)_3Cl$ moiety, resulting in red shift in the emission maxima and substantial quenching in the emission intensity. A red shift in the emission wavelength was also observed for $[Ru(dceb)_2(Hbpt)Re(CO)_3Cl](PF_6)_2$ (at 688 nm) compared with $[Ru(dceb)_2(Hbpt)](PF_6)_2$ (at 627 nm).

4.5 Photocatalytic Studies

A number of the complexes presented in this section were studied for their ability to produce hydrogen photochemically. Surprisingly, no evidence for the formation of hydrogen was obtained; however, these complexes were found to reduce carbon dioxide photocatalytically using both intramolecular and intermolecular approaches. Products obtained included formate and carbon monoxide.

Figures 4.8–4.10 show the TONs for the products observed, namely carbon monoxide and formate.

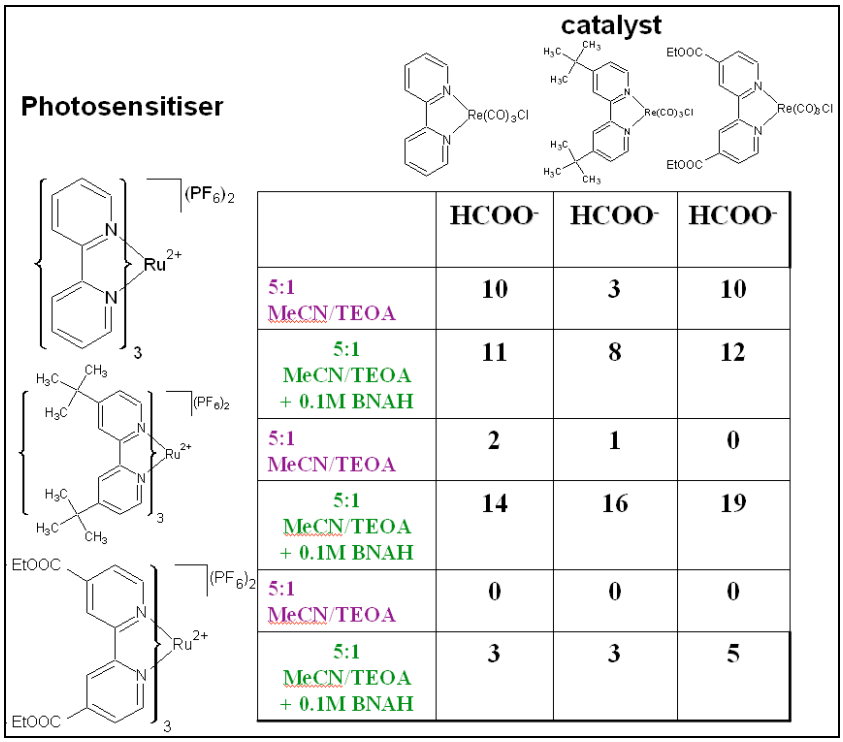

	HCOO⁻	HCOO⁻	HCOO⁻
5:1 MeCN/TEOA	10	3	10
5:1 MeCN/TEOA + 0.1M BNAH	11	8	12
5:1 MeCN/TEOA	2	1	0
5:1 MeCN/TEOA + 0.1M BNAH	14	16	19
5:1 MeCN/TEOA	0	0	0
5:1 MeCN/TEOA + 0.1M BNAH	3	3	5

Figure 4.8. TONs for the production of formate following the photolysis of ruthenium sensitisers with various catalysts.

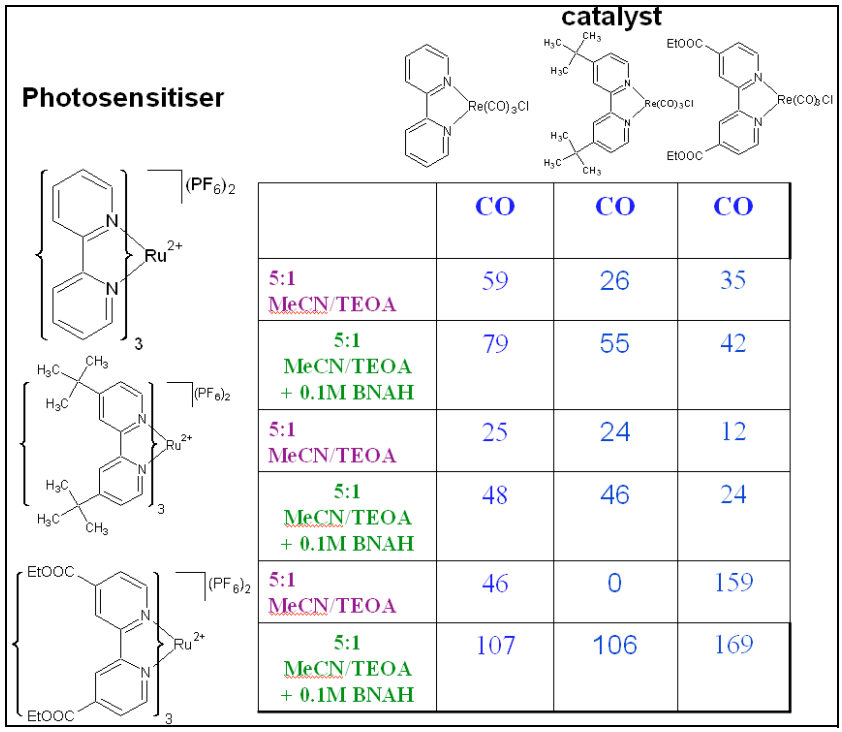

	CO	CO	CO
5:1 MeCN/TEOA	59	26	35
5:1 MeCN/TEOA + 0.1M BNAH	79	55	42
5:1 MeCN/TEOA	25	24	12
5:1 MeCN/TEOA + 0.1M BNAH	48	46	24
5:1 MeCN/TEOA	46	0	159
5:1 MeCN/TEOA + 0.1M BNAH	107	106	169

Figure 4.9. TONs for the production of carbon monoxide following the photolysis of ruthenium sensitisers with various catalysts.

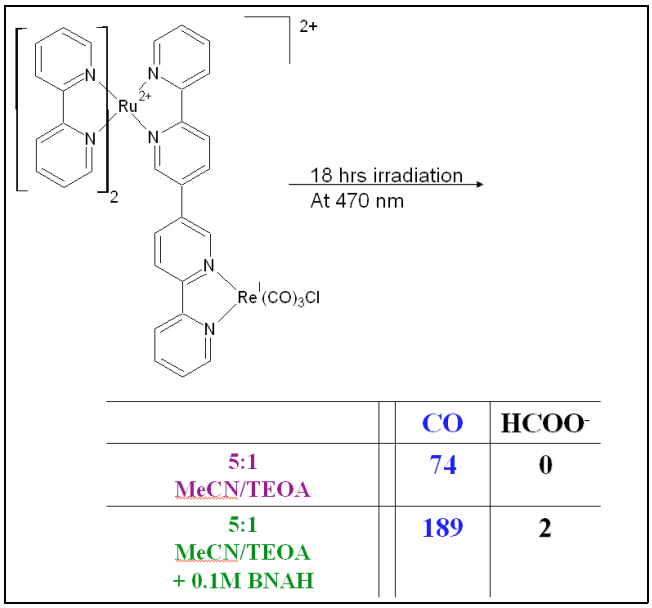

	CO	$HCOO^-$
5:1 MeCN/TEOA	74	0
5:1 MeCN/TEOA + 0.1M BNAH	189	2

Figure 4.10. Intramolecular studies for the production of formate and carbon monoxide.

5 Conclusions

This study has identified both inorganic and organic molecules that produce hydrogen efficiently. In this project, in the order of 50 compounds were synthesised and characterised, some of which are discussed in this report. Detailed photocatalytic studies were carried out as a function of the chemical composition of the compounds, as well as of the catalytic conditions. In these studies, both intramolecular and intermolecular approaches were applied. The results obtained show that in most cases the intramolecular approach yielded the best results. In these studies, TONs of up to 500 per 8 h were obtained for the formation of hydrogen using iridium-based complexes. Surprisingly, while the iridium compounds produced considerable amounts of hydrogen, the ruthenium compounds produced no hydrogen; however, the compounds were shown to be able to reduce carbon dioxide to mainly carbon monoxide and small amounts of formic acid, compounds that can be used for energy purposes or as a feedstock for industry. In this manner, carbon dioxide can be recycled, which would be very beneficial in the fight to stop climate change.

In order to achieve the full environmental benefit of hydrogen as an energy carrier, low-carbon-intensive, low-polluting and lower-cost processes for producing hydrogen from renewable energy sources must be developed. This project has demonstrated that it is possible to produce hydrogen using visible light irradiation, and the first step has been taken towards the development of a green approach to carbon dioxide reduction and recycling. In the Irish context, the development of the environment-friendly production methods will provide employment and the potential for exporting this technology all over the world.

6 Peer-Reviewed Publications to Date

The following is a list of the peer-reviewed publications to for the work funded by 2008-ET-MS-3-S2 – *The Design of New Photocatalytic Systems for the Generation of Hydrogen from Water Using Solar Energy*.

Inglis, J.L., MacLean, B.J., Pryce, M.T. and Vos, J.G., 2012. Electrocatalytic pathways towards sustainable fuel production from water and CO_2. *Coordination Chemistry Reviews* **256(21–22):** 2571–2600.

Paul, A., Connolly, D., Schulz, M., Pryce, M.T. and Vos, J.G., 2012. Effect of water during the quantitation of formate in photocatalytic studies on CO_2 reduction in dimethylformamide. *Inorganic Chemistry* **51:** 1977–1979.

Schulz, M., Hirschmann, J., Draksharapu, A., Singh Bindra, G., Soman, S., Paul, A., Groarke, R., Pryce, M.T., Rau, S., Browne, W.R. and Vos, J.G., 2011. Reinvestigating 2,5-di(pyridin-2-yl)pyrazine ruthenium complexes: selective deuteration and Raman spectroscopy as tools to probe ground and excited-state electronic structure in homo- and heterobimetallic complexes. *Dalton Transactions* **40:** 10545–10552.

Singh Bindra, G., Schulz, M., Paul, A., Groarke, R., Soman, S., Inglis, J.L., Browne, W.R., Pfeffer, M.G., Rau, S., MacLean, B.J., Pryce, M.T. and Vos, J.G., 2012. The role of bridging ligand in hydrogen generation by photocatalytic Ru/Pd assemblies. *Dalton Transactions* **41:** 13050–13059.

Singh Bindra, G., Schulz, M., Paul, A., Soman, S., Groarke, R., Inglis, J., Pryce, M.T., Browne, W.R., Rau, S., Maclean, B.J. and Vos, J.G., 2011. The effect of peripheral bipyridine ligands on the photocatalytic hydrogen production activity of Ru/Pd catalysts. *Dalton Transactions* **40:** 10812–10814.

Soman, S., Singh Bindra, G., Paul, A., Groarke, R., Manton, J.C., Connaughton, F.M., Schulz, M., Dini, D., Long, C., Pryce, M.T. and Vos, J.G., 2012. Wavelength dependent photocatalytic H_2 generation using Iridium-Pt/Pd complexes. *Dalton Transactions* **41:** 12678–12680.

References

Adler, A.D., Longo, F.R., Finarelli, J.D., Goldmacher, J., Assour, J. and Korsalioff, L., 1967. A simplified synthesis for meso-tetraphenylporphine. *Journal of Organic Chemistry* **32(2):** 476–476.

Amouyal, E., Zidler, B., Keller, P. and Moradpour, A., 1980. Excited-state electron-transfer quenching by a series of water photoreduction mediators. *Chemical Physics Letters* **74(2):** 314–317.

Andreiadis, E.S., Kerlidou, M.C., Fontecave, M. and Artero, V., 2011. Artificial photosynthesis: from molecular catalysts for light-driven water splitting to photoelectrochemical cells. *Photochemistry and Photobiology* **87(5):** 946–964.

Armaroli, N. and Balzani, V., 2007. The future of energy supply: challenges and opportunities. *Angewandte Chemie International Edition* **46(1–2):** 52–66.

Bardwell, D.A., Barigelletti, F., Cleary, R.L., Flamigni, L., Guardigli, M., Jeffery, J.C. and Ward, M.D., 1995. Synthesis, electrochemical behavior, and spectroscopic and luminescence properties of dinuclear species containing $[Ru(diimine)3]^{2+}$ and $[Re(diimine)Cl(CO)_3]$ chromophores bridged by a nonsymmetric quaterpyridine ligand. *Inorganic Chemistry* **34(5):** 2438–2446.

Bian, Z.-Y., Sumi, K., Furue, M., Sato, S., Koike, K. and Ishitani, O., 2008. A novel tripodal ligand, Tris[(4'-methyl-2,2'-bipyridyl-4-yl)methyl]carbinol and its trinuclear Ru^{II}/Re^{I} mixed-metal complexes: synthesis, emission properties, and photocatalytic CO_2 reduction. *Inorganic Chemistry* **47(23):** 10801–10803.

Bian, Z.Y., Sumi, K., Furue, M., Sato, S., Koike, K. and Ishitani, O., 2009. Synthesis and properties of a novel tripodal bipyridyl ligand tb-carbinol and its Ru(II)-Re(I) trimetallic complexes: investigation of multimetallic artificial systems for photocatalytic CO_2 reduction. *Dalton Transactions* **6:** 983–993.

Brown, G.M., Chan, S.F., Creutz, C., Schwarz, H.A. and Sutin, N., 1979. Mechanism of the formation of dihydrogen from the photoinduced reactions of tris(bipyridine)ruthenium(II) with tris(bipyridine) rhodium(III). *Journal of the American Chemical Society* **101(25):** 7638–7640.

Chan, S.F., Chou, M., Creutz, C., Matsubara, T. and Sutin, N., 1981. Mechanism of the formation of dihydrogen from the photoinduced reactions of poly(pyridine)ruthenium(II) and poly(pyridine) rhodium(III) complexes. *Journal of the American Chemical Society* **103(2):** 369–379.

Chan, W.K., Hui, C.S., Man, K.Y.K., Cheng, K.W., Wong, H.L., Zhu, N. and Djurisic, A.B., 2005. Synthesis and photosensitizing properties of conjugated polymers that contain chlorotricarbonyl bis(phenylimino) acenaphthene rhenium(I) complexes. *Coordination Chemistry Reviews* **249(14):** 1351–1359.

Chiorboli, C., Rodgers, M.A.J. and Scandola, F., 2003. ultrafast processes in bimetallic dyads with extended aromatic bridges. energy and electron transfer pathways in tetrapyridophenazine-bridged complexes. *Journal of the American Chemical Society* **125(2):** 483–491.

Coe, B.J., Curati, N.R.M., Fitzgerald, E.C., Coles, S.J., Horton, P.N., Light, M.E. and Hursthouse, M.B., 2007. Syntheses and properties of bimetallic chromophore-quencher assemblies containing ruthenium(II) and rhenium(I) centers. *Organometallics* **26(9):** 2318–2329.

Coleman, A., Brennan, C., Vos, J.G. and Pryce, M.T., 2008. Photophysical properties and applications of Re(I) and Re(I)–Ru(II) carbonyl polypyridyl complexes. *Coordination Chemistry Reviews* **252(23):** 2585–2595.

Colombo, M.G., Hauser, A. and Gudel, H.U., 1993. Evidence for strong mixing between the LC and MLCT excited states in bis(2-phenylpyridinato-C2,N')(2,2'-bipyridine)iridium(III). *Inorganic Chemistry* **32(14):** 3088.

Colombo, M.G., Hauser, A. and Gudel, H.U., 1994. *In:* Yersin H (Ed.) Electronic and vibronic spectra of transition metal complexes. Vol. I. *Topics in Current Chemistry* 171. Springer, Berlin Heidelberg, New York, USA, p. 143.

Constable, E.C. and Seddon, K.R., 1982. A deuterium exchange reaction of the tris-(2,2'-bipyridine)ruthenium(II) cation: evidence for the acidity of the 3,3'-protons. *Journal of the Chemical Society, Chemical Communications* **1:** 34–36.

Currao, A., Reddy, V.R., Veen, M.K.V., Schropp, R.E.I. and Calzaferri, G., 2004. Water splitting with silver chloride photoanodes and amorphous silicon solar cells. *Photochemistry and Photobiology Sciences* **3(12):** 1017–1025.

DeLaive, P.J., Sullivan, B.P., Meyer, T.J. and Whitten, D.G., 1979. Applications of light-induced electron-transfer reactions. Coupling of hydrogen generation with photoreduction of ruthenium(II) complexes by triethylamine. *Journal of the American Chemical Society* **101(14):** 4007–4008.

Dhanasekaran, T., Grodkowski, J., Neta, P., Hambright,

P. and Fujita, E., 1999. p-Terphenyl-sensitized photoreduction of CO_2 with cobalt and iron porphyrins. Interaction between CO and reduced metalloporphyrins. *Journal of Physical Chemistry A* **103(38):** 7742–7748.

Dietzek, B., Kiefer, W., Blumhoff, J., Mttcher, L.B., Rau, S., Walther, D., Uhlemann, U., Schmitt, M. and Popp, J., 2006. Ultrafast excited-state excitation dynamics in a quasi-two-dimensional light-harvesting antenna based on ruthenium(II) and palladium(II) chromophores. *Chemistry – A European Journal* **12(19):** 5105–5155.

Doherty, M.D., Grills, D.C., Muckerman, J.T., Polyansky, D.E. and Fujita, E., 2009. Toward more efficient photochemical CO_2 reduction: Use of $scCO_2$ or photogenerated hydrides. *Coordination Chemistry Reviews* **254 (21):** 2472.

Edwards, P.P., Kuznetsov, V.L. and David, W.I.F., 2007. Hydrogen energy. *Philosophical Transactions of the Royal Society A* **365(1853):** 1043.

Eisenberg, R. and Nocera, D.G., 2005. Preface: overview of the forum on solar and renewable energy. *Inorganic Chemistry* **44(20):** 6799.

Encinas, S., Barthram, A.M., Ward, M.D., Barigelletti, F. and Campagna, S., 2001. Photoinduced two-step energy transfer in a Re/Ru dinuclear complex as mediated by an interposed 'reservoir' unit. *Chemical Communications* **3:** 277–278.

Esswein, A.J. and Nocera, D.G., 2007. Hydrogen production by molecular photocatalysis. *Chemical Reviews* **107(10):** 4022–4047.

Ettedgui, J., Diskin-Posner, Y., Weiner, L. and Neumann, R., 2011. Photoreduction of carbon dioxide to carbon monoxide with hydrogen catalyzed by a rhenium(I) phenanthroline-polyoxometalate hybrid complex. *Journal of the American Chemical Society* **133(2):** 188–190.

Ewan, B.C.R. and Allen, R.W.K., 2005. A figure of merit assessment of the routes to hydrogen. *International Journal of Hydrogen Energy* **30(8):** 809.

Ferreira, K.N., Iverson, T.M., Maghlaoui, K., Barber, J. and Iwata, S., 2004. Architecture of the photosynthetic oxygen-evolving center. *Science* **303(5665):** 1831.

Fihri, A., Artero, V., Pereira, A. and Fontecave, M., 2008a. Efficient H_2-producing photocatalytic systems based on cyclometalated iridium- and tricarbonylrhenium-diimine photosensitizers and cobaloxime catalysts. *Dalton Transactions* **41:** 5567–5569.

Fihri, A., Artero, V., Razavet, M., Baffert, C., Leibl, W. and Fontecave, M., 2008b. Cobaloxime-based photocatalytic devices for hydrogen production. *Angewandte Chemie International Edition* **47(3):** 564–567.

Fraser, M.G., Clark, C.A., Horvath, R., Lind, S.J., Blackman, A.G., Sun, X.-Z., George, M.W. and Gordon, K.C., 2011. Complete family of mono-, bi-, and trinuclear $ReI(CO)_3Cl$ complexes of the bridging polypyridyl ligand 2,3,8,9,14,15-Hexamethyl-5,6,11,12,17,18-hexaazatrinapthalene: syn/anti isomer separation, characterization, and photophysics. *Inorganic Chemistry* **50(13):** 6093–6106.

Fujishima, A. and Honda, K., 1971. Electrochemical evidence for the mechanism of the primary stage of photosynthesis. *Bulletin of the Chemical Society of Japan* **44:** 1148–1150.

Fujishima, A. and Honda, K., 1972. Electrochemical photolysis of water at a semiconductor electrode. *Nature* **238(5358):** 37–38.

Gholamkhass, B., Mametsuka, H., Koike, K., Tanabe, T., Furue, M. and Ishitani, O., 2005. Architecture of supramolecular metal complexes for photocatalytic CO_2 reduction: ruthenium-rhenium bi- and tetranuclear complexes. *Inorganic Chemistry* **44(7):** 2326–2336.

Goldsmith, J.I., Hudson, W.R., Lowry, M.S., Anderson, T.H. and Bernhard, S., 2005. Discovery and high-throughput screening of heteroleptic iridium complexes for photoinduced hydrogen production. *Journal of the American Chemical Society* **127(20):** 7502–7510.

Grätzel, M., 1981. Artificial photosynthesis: water cleavage into hydrogen and oxygen by visible light. *Accounts of Chemical Research* **14(12):** 376–384.

Hawecker, J., Lehn, J.M. and Ziessel, R., 1983a. Efficient photochemical reduction of CO_2 to CO by visible light irradiation of systems containing $Re(bipy)(CO)_3X$ or $Ru(bipy)3^{2+}$–Co^{2+} combinations as homogeneous catalysts. *Nouveau Journal de Chimie* **7:** 271–301.

Hawecker, J., Lehn, J.-M. and Ziessel, R., 1983b. Efficient photochemical reduction of CO_2 to CO by visible light irradiation of systems containing $Re(bipy)(CO)_3X$ or $Ru(bipy)\ 3^{2+}$–Co^{2+} combinations as homogeneous catalysts. *Journal of the Chemical Society, Chemical Communications* **9:** 536–538.

Hay, P.J., 2002. Theoretical studies of the ground and excited electronic states in cyclometalated phenylpyridine Ir(III) complexes using density functional theory. *Journal of Physical Chemistry A* **106(8):** 1634–1641.

Hayashi, Y., Kita, S., Brunschwig, B.S. and Fujita, E., 2003. Involvement of a Binuclear Species with the Re-C(O)O-Re Moiety in CO_2 reduction catalyzed by tricarbonyl rhenium(I) complexes with diimine ligands: strikingly slow formation of the Re-Re and Re-C(O)O-Re species from Re(dmb)(CO)3S (dmb = 4,4'-

Dimethyl-2,2'-bipyridine, S = Solvent). *Journal of the American Chemical Society* 125 **(39):** 11976–11987.

Hosono, H. and Kaneko, M., 1997. Effect of configuration of viologen-linked porphyrin on photocurrent generation and on photoinduced hydrogen evolution. *Journal of the Chemical Society, Faraday Transactions* **93(7):** 1313–1319.

Ioachim, E., Medlycott, E.A. and Hanan, G.S., 2006. Synthesis and properties of Re(I) tricarbonyl complexes of 6,6'-disubstituted-4,4'-bipyrimidines with high energy excited states suitable for incorporation into polynuclear arrays. *Inorganica Chimica Acta* **359(9):** 2599–2607.

Ishitani, O., George, M.W., Ibusuki, T., Johnson, F.P.A., Koike, K., Nozaki, K., Pac, C., Turner, J.J. and Westwell, J.R., 1994. Photophysical behavior of a new CO_2 reduction catalyst, $Re(CO)_2(bpy)\{P(OEt)_3\}^{2+}$. *Inorganic Chemistry* **33(21):** 4712–4717.

Ishitani, O., Kanai, K., Yamada, Y. and Sakamoto, K., 2001. Synthesis of a linear-shaped tetramer and trimers of rhenium(I) diimine complexes. *Chemical Communications* **16:** 1514–1515.

Jacobson, M.Z., Colella, W.G. and Golden, D.M., 2005. Cleaning the air and improving health with hydrogen fuel-cell vehicles. *Science* **308(5730):** 1901.

Jasimuddin, S., Yamada, T., Fukuju, K, Otsaki, J. and Sakai, K., 2010. Photocatalytic hydrogen production from water in self-assembled supramolecular iridium–cobalt systems. *Chemical Communications* **46(44):** 8466–8468.

Kalyanasundaram, K., 1992. *Photochemistry of Polypyridine and Porphyrin Complexes*. Academic Press, New York, NY, USA. p. 105.

Kalyanasundaram, K. and Nazeeruddin, M.K., 1990. Ligand-bridged homo- and hetero-binuclear carbonyl polypyridyl complexes of ReI: syntheses, electronic spectra, redox, and luminescence behaviour. *Journal of the Chemical Society, Dalton Transactions* **5:** 1657–1662.

Kalyanasundaram, K., Kiwi, J. and Grätzel, M., 1978. Hydrogen evolution from water by visible light, a homogeneous three component test system for redox catalysis. *Helvetica Chimica Acta* **61(7):** 2720–2730.

Kalyanasundaram, K., Graetzel, M. and Nazeeruddin, M.K., 1992. Luminescence and intramolecular energy-transfer processes in isomeric cyano-bridged rhenium(I)-rhenium(I) and rhenium(I)-ruthenium(II)-rhenium(I) polypyridyl complexes. *Inorganic Chemistry* **31(25):** 5243–5253.

Kirch, M., Lehn, J.M. and Sauvage, J.P., 1979. Hydrogen generation by visible light irradiation of aqueous solutions of metal complexes. An approach to the photochemical conversion and storage of solar energy. *Helvetica Chimica Acta* **62(4):** 1345–1384.

Kobayashi, A., Sakamoto, K. and Ishitani, O., 2005. Reaction of an NAD(P)+ model compound coordinated to a transition metal complex with ruthenium and rhenium hydrido complexes. *Inorganic Chemistry Communications* **8(4):** 365–367.

Konno, H., Kobayashi, A., Sakamoto, K., Fagalde, F., Katz, N.E., Saitoh, H. and Ishitani, O., 2000. Synthesis and properties of $[Ru(tpy)(4,4'\text{-}X_2bpy)H]^+$ (tpy=2,2':6',2-terpyridine, bpy=2,2'-bipyridine, X=H and MeO), and their reactions with CO_2. *Inorganica Chimica Acta* **299(2):** 155–163.

Konno, H., Ishii, Y., Sakamoto, K. and Ishitani, O., 2002. Synthesis, spectroscopic characterization, electrochemical and photochemical properties of ruthenium(II) polypyridyl complexes with a tertiary amine ligand. *Polyhedron* **21(1):** 61–68.

Krishnan, C.V. and Sutin, N., 1981. Homogeneous catalysis of the photoreduction of water by visible light. 2. Mediation by a tris(2,2'-bipyridine)ruthenium(II)-cobalt(II) bipyridine system. *Journal of the American Chemical Society* **103(8):** 2141–2142.

Krishnan, C.V., Brunschwig, B.S., Creutz, C. and Sutin, N., 1985. Homogeneous catalysis of the photoreduction of water. 6. Mediation by polypyridine complexes of ruthenium(II) and cobalt(II) in alkaline media. *Journal of the American Chemical Society* **107(7):** 2005–2015.

Lam, L.S.M., Chan, W.K., Djurisic, A.B. and Herbert Li, E., 2002. Study of charge generation process in some photosensitizing rhenium diimine complexes. *Chemical Physics Letters* **362(1):** 130–134.

Lazarides, T., Barbieri, A., Sabatini, C., Barigelletti, F., Adams, H. and Ward, M.D., 2007. Photoinduced energy transfer between Re(I) and Ru(II) termini connected through a new exo-ditopic bis-phenanthroline ligand fused to a central macrocycle spacer: synthesis, structure, and electrochemical and photophysical properties of a heterodinuclear complex. *Inorganica Chimica Acta* **360(3):** 814–824.

Lehn, J.M. and Sauvage, J.P., 1977. Chemical storage of light energy: Catalytic generation of hydrogen by visible light or sunlight irradiation of neutral aqueous solutions. *Nouveau Journal de Chimie* **1:** 449–451.

Lewis, N.S. and Nocera, D.G., 2006. Powering the planet: chemical challenges in solar energy utilization. *Proceedings of the National Academy of Sciences of the United States of America* **103(43):** 15729.

Linkous, C.A., 1992. Hydrogen energy progress IX. *Proceedings of the Ninth World Hydrogen Energy Conference*. Pergamon Press, Paris, France). p. 419.

Losse, S., Vos, J.G. and Rau, S., 2010. Catalytic

hydrogen production at cobalt centres. *Coordination Chemistry Reviews* **254(21):** 2492–2504.

Lowry, M.S., Goldsmith, J.I., Slinker, J.D., Rohl, R., Pascal, R.A., Malliaras, G.G. and Bernhard, S., 2005. Single-layer electroluminescent devices and photoinduced hydrogen production from an ionic iridium(III) complex. *Chemistry of Materials* **17(23):** 5712–5719.

McEvoy, J.P. and Brudvig, G.W., 2006. Water-splitting chemistry of Photosystem II. *Chemical Reviews* **106(11):** 4455–4483.

Nelson, N. and Shem, A.B., 2004. The complex architecture of oxygenic photosynthesis. *Nature Reviews Molecular Cell Biology* **5:** 971–982.

Oyama, D., Kobayashi, T., Shiren, K. and Tanaka, K., 2003. Regulation of electron donating ability to metal center: isolation and characterization of ruthenium carbonyl complexes with N,N- and/or N,O-donor polypyridyl ligands. *Journal of Organometallic Chemistry* **665:** 107–113.

Ozawa, H., Haga, M. and Sakai, K., 2006. A photo-hydrogen-evolving molecular device driving visible-light-induced EDTA-reduction of water into molecular hydrogen. *Journal of the American Chemical Society* **128(15):** 4926–4927.

Penner, S.S., 2006. Steps toward the hydrogen economy. *Energy* **31(1):** 33–43.

Polson, M., Fracasso, S., Bertolasi, V., Ravaglia, M. and Scandola, F., 2004. Iridium cyclometalated complexes with axial symmetry. synthesis and photophysical properties of a trans-biscyclometalated complex containing the terdentate ligand 2,6-diphenylpyridine. *Inorganic Chemistry* **43(6):** 1950.

Possamai, G., Menna, E., Maggini, M., Carano, M., Marcaccio, M., Paolucci, F., Guldi, D.M. and Swartz, A., 2006. Rhenium(I) and ruthenium(II) complexes with a crown-linked methanofullerene ligand: synthesis, electrochemistry and photophysical characterization. *Photochemical & Photobiological Sciences* **5(12):** 1154–1164.

Rau, S., Schäfer, B., Gleich, D., Anders, E., Rudolph, M., Friedrich, M., Görls, H., Henry, W. and Vos, J.G., 2006. A supramolecular photocatalyst for the production of hydrogen and the selective hydrogenation of tolane. *Angewandte Chemie International Edition* **45(37):** 6215–6218.

Rau, S., Walther, D. and Vos, J.G., 2007. Inspired by nature: light driven organometallic catalysis by heterooligonuclear Ru(II) complexes. *Dalton Transactions* **9:** 915–919.

Riklin, M., Tran, D., Bu, X., Laverman, L.E. and Ford, P.C., 2001. The synthesis of the ligand 1,5-bis[2-(3,5-dimethyl-1-pyrazolyl)ethyl]-amine-1,10-phenanthroline) and of its ruthenium(II) and rhenium(I) complexes. Binuclear species with Cu(I) and Cu(II) and some photophysical properties. *Journal of the Chemical Society*, *Dalton Transactions* **12:** 1813–1819.

Rillema, D.P., Sahai, R., Matthews, P., Edwards, A.K., Shaver, R.J. and Morgan, L., 1990. Utility of the semiempirical INDO/1 method for the calculation of the geometries of second-row transition-metal species. *Inorganic Chemistry* **29(1):** 1–3.

Rodat, S., Abanades, S., Sans, J.L. and Flamant, G., 2010. A pilot-scale solar reactor for the production of hydrogen and carbon black from methane splitting. *International Journal of Hydrogen Energy* **35(15):** 7748.

Roeb, M., Neises, M., Sack, J., Rietbrock, P., Monnerie, N., Dersch, J., Schmitz, M. and Sattler, C., 2009. Operational strategy of a two-step thermochemical process for solar hydrogen production. *International Journal of Hydrogen Energy* **34(10):** 4537.

Sahai, R, Rillema, D.P., Shaver, R., Van Wallendael, S., Jackman, D.C. and Boldaji, M., 1989. Complexes of ruthenium(II) with (2,2'-bipyrimidine) tricarbonylchlororhenium and {benzo[1,2-6:3,4-b':5,6-b"]tripyrazine}hexacarbonyldichloridirhenium as ligands: syntheses and redox and luminescence properties. *Inorganic Chemistry* **28(6):** 1022.

Sato, S., Morimoto, T. and Ishitani, O., 2007. Photochemical synthesis of mer-[Re(bpy)$(CO)_3$Cl]. *Inorganic Chemistry* **46(22):** 9051–9053.

Schulz, M., Hirschmann, J., Draksharapu, A., Singh Bindra, G., Soman, S., Paul, A., Groarke, R., Pryce, M.T., Rau, S., Browne, W.R. and Vos, J.G., 2011. Reinvestigating 2,5-di(pyridin-2-yl)pyrazine ruthenium complexes: selective deuteration and Raman spectroscopy as tools to probe ground and excited-state electronic structure in homo- and heterobimetallic complexes. *Dalton Transactions* **40(40):** 10545–10553.

Sherif, S.A., Barbir, F. and Veziroglu, T.N., 2005. Wind energy and the hydrogen economy-review of the technology. *Solar Energy* **78(5):** 647–660.

Sigfusson, T.I., 2007. Pathways to hydrogen as an energy carrier. *Philosophical Transactions of the Royal Society A* **365(1853):** 1025–1042.

Simpson, T.J. and Gordon, K.C., 1995. Spectroscopic and electrochemical studies of rhenium(I) bimetallic complexes with asymmetric polypyridyl bridging ligands. *Inorganic Chemistry* **34(25):** 6323–6329.

Singh, S.P., Srivastava, S.C. and Pandey, K.D., 1990. Photoproduction of hydrogen by a non-sulphur bacterium isolated from root zones of water fern *Azolla pinnata*. *International Journal of Hydrogen Energy* **15(6):** 403–406.

Singh Bindra, G., 2012. *Light Driven Hydrogen*

Generation by Ruthenium(II) – Palladium(II) / Platinum(II) Supramolecular Photocatalysts Using Water. PhD Thesis, Dublin City University, Dublin, Ireland.

Singh Bindra, G.S., Shulz, M., Paul, A., Soman, S., Groarke, R., Inglis, J., Pryce, M.T., Browne, W.R., Rau, S., Maclean, B.J. and Vos, J.G., 2011. The effect of peripheral bipyridine ligands on the photocatalytic hydrogen production activity of Ru/Pd catalysts. *Dalton Transactions* **40(41):** 10812–10814.

Slinker, J.D., Goroddetsky, A.A., Lowry, M.S., Wang, J., Parker, S., Rohl, R., Bernhard, S. and Malliaras, G.G., 2004. Efficient yellow electroluminescence from a single layer of a cyclometalated iridium complex. *Journal of the American Chemical Society* **126(9):** 2763–2767.

Stufkens, D.J. and Vlcek, A., 1998. Ligand-dependent excited state behaviour of Re(I) and Ru(II) carbonyl–diimine complexes. *Coordination Chemistry Reviews* **177(1):** 127–179.

Takeda, H. and Ishitani, O., 2009. Development of efficient photocatalytic systems for CO_2 reduction using mononuclear and multinuclear metal complexes based on mechanistic studies. *Coordination Chemistry Reviews* **254(4):** 346–354.

Takeda, H., Koike, K., Inoue, H. and Ishitani, O., 2008. Development of an efficient photocatalytic system for CO_2 reduction using rhenium(I) complexes based on mechanistic studies. *Journal of the American Chemical Society* **130(7):** 2023–2031.

Takeda, H., Ohashi, M., Tani, T., Ishitani, O. and Inagaki, S., 2010. Enhanced photocatalysis of rhenium(I) complex by light-harvesting periodic mesoporous organosilica. *Inorganic Chemistry* **49(10):** 4554–4559.

Turner, J.A., 2004. Sustainable hydrogen production. *Science* **305(5686):** 972.

Turner, J., Sverdrup, G., Mann, M.K., Maness, P.C., Kroposki, B., Ghirardi, M., Evans, R.J. and Blake, D., 2008. Renewable hydrogen production. *International Journal of Energy Research* **32(5):** 379.

Van Wallendael, S., Shaver, R.J., Rillema, D.P., Yoblinski, B.J., Stathis, M. and Guarr, T.F., 1990. Ground-state and excited-state properties of monometallic and bimetallic complexes based on rhenium(I) tricarbonyl chloride: effect of an insulating vs. a conducting bridge. *Inorganic Chemistry* **29(6):** 1761–1767.

Velayudham, M. and Rajagopal, S., 2009. Synthesis, characterization, photophysics and intramolecular energy transfer process in bimetallic rhenium(I)–ruthenium(II) complexes. *Inorganica Chimica Acta* **362(14):** 5073–5079.

Velayudham, M., Singaravadivel, S., Rajagopal, S. and Ramamurthy, P., 2009. Synthesis, characterization and photophysics of alkyne bridged bimetallic rhenium(I) and ruthenium(II) complexes. *Journal of Organometallic Chemistry* **694(25):** 4076–4083.

Vogler, A. and Kisslinger, J., 1986. Bipyrimidine-bridged rhenium(I)/rhenium(I) and ruthenium(II)/rhenium(I) complexes. Synthesis, electronic absorption and emission spectra. *Inorganica Chimica Acta* **115(2):** 193–196.

Waterland, R., Simpson, M.J., Gordon, K.C. and Burrell, A.K., 1998. Spectroelectrochemical studies and excited-state resonance-Raman spectroscopy of some mononuclear rhenium(I) polypyridyl bridging ligand complexes. Crystal structure determination of tricarbonylchloro[2,3-di(2-pyridyl)quinoxaline]rhenium (I). *Journal of the Chemical Society*, *Dalton Transactions* **1:** 185–192.

Watts, R.J. and Van Houten, J.V., 1974. Effect of ligand substituents of the d-d luminescence of iridium(III) and rhodium(III) complexes of 1,10-phenanthroline. *Journal of the American Chemical Society* **96(13):** 4334–4335.

Worl, L.A., Duesing, R., Chen, P., Ciana, L.D. and Meyer, T.J., 1991. Photophysical properties of polypyridyl carbonyl complexes of rhenium(I). *Journal of the Chemical Society*, *Dalton Transactions* **S:** 849–854.

Wrighton, M.S. and Morse, D.L., 1974. Nature of the lowest excited state in tricarbonylchloro-1,10-phenanthrolinerhenium(I) and related complexes. *Journal of the American Chemical Society* **96(4):** 998–1004.

Yamamoto, Y., Sawa, S., Funada, Y., Morimoto, T., Falkenstrom, M., Miyasaka, H., Shishido, S., Ozeki, T., Koike, K. and Ishitani, O., 2008. Systematic synthesis, isolation, and photophysical properties of linear-shaped Re(I) oligomers and polymers with 2-20 units. *Journal of the American Chemical Society* **130(44):** 14659–14674.

Yamamoto, Y., Tamaki, Y., Yui, T., Koike, K., Ishitani, O., 2010. New light-harvesting molecular systems constructed with a Ru(II) complex and a linear-shaped Re(I) oligomer. *Journal of the American Chemical Society* **132(33):** 11743–11752.

Zhang, P., Wang, M., Li, C., Li, X., Dong, J. and Sun, L., 2010. Photochemical H_2 production with noble-metal-free molecular devices comprising a porphyrin photosensitizer and a cobaloxime catalyst. *Chemical Communications* **46(45):** 8806–8808.

Zhu, M., Lu, Y., Du, Y., Li, J., Wang, X. and Yang, P., 2011. Photocatalytic hydrogen evolution without an electron mediator using a porphyrin–pyrene conjugate functionalized Pt nanocomposite as a photocatalyst. *International Journal of Hydrogen Energy* **36(7):** 4298–4304.

Ziessel, R., Juris, A. and Venturi, M., 1997. A new

rhenium(I) tricarbonylpolypyridine donor–acceptor complex featuring a long-lived charge-separated excited state. *Chemical Communications* **17:** 1593–1594.

Ziessel, R., Juris, A. and Venturi, M., 1998. Intramolecular photoinduced electron transfer in multicomponent rhenium(I) donor–acceptor complexes. *Inorganic Chemistry* **37(20):** 5061–5069.

Acronyms

ACN	Acetonitrile
ATP	Adenosine triphosphate
bpm	2,2-Bipyrimidine
bpp	2-(6-(Pyridin-2-yl)pyridin-3-yl)pyridine)
CB	Conduction band
Co	Cobalt
CO	Carbon monoxide
CO_2	Carbon dioxide
CoTPP	Cobalt(II) tetraphenylporphyrin (CoTPP)
DCM	Dichloromethane
dpp	2,5-di(Pyridin-2-yl)pyrazine
EDTA	Ethylenediaminetetraacetic acid
EtOH	Ethanol
FeTPP	Iron(II)-tetraphenylporphyrin
FID	Flame ionisation detector
H_2PtCl_6	Platinum hexachloride
HOMO	Highest occupied molecular orbital
Ir	Iridium
K_2PdCl_4	Potassium tetrachloropallidate
K_2PtCl_4	Potassium tetrachloroplatinate(II)
KPF_6	Potassium hexafluorophosphate
LB	Langmuir–Blodgett
LC	Ligand centred
LFSE	Ligand field stabilisation energy
LLCT	Ligand-to-ligand centred transition
LUMO	Lowest unoccupied molecular orbital
MeOH	Methanol
MLCT	Metal-to-ligand charge transfer
MPyTPP	5-Pyridyl-15,20,25-triphenylporphyrin
NADPH	Nicotinamide adenine dinucleotide phosphate
NH	Amine hydrogen
$(NH_4)_2PdCl_4$	Ammonium tetrachloropalladate(II)

^{3}MC	Triplet metal-centred
NMR	Nuclear magnetic resonance
OLED	Organic light-emitting diode
Pd	Palladium
PS	Photosensitiser
PSI	Photosystem I
PSII	Photosystem II
Pt	Platinum
Re	Rhenium
Ru	Ruthenium
SEM	Scanning electron microscopy
SR	Sacrificial reductant
TCD	Thermal conductivity detector
TEA	Triethylamine
TEM	Transmission electron microscopy
TEOA	Triethanolamine
THF	Tetrahydrofuran
TON	Turnover number
tpy	2,2:6,2-Terpyridine
UV	Ultraviolet
VB	Valence band
Zn	Zinc

An Ghníomhaireacht um Chaomhnú Comhshaoil

Is í an Gníomhaireacht um Chaomhnú Comhshaoil (EPA) comhlachta reachtúil a chosnaíonn an comhshaol do mhuintir na tíre go léir. Rialaímid agus déanaimid maoirsiú ar ghníomhaíochtaí a d'fhéadfadh truailliú a chruthú murach sin. Cinntímid go bhfuil eolas cruinn ann ar threochtaí comhshaoil ionas go nglactar aon chéim is gá. Is iad na príomh-nithe a bhfuilimid gníomhach leo ná comhshaol na hÉireann a chosaint agus cinntiú go bhfuil forbairt inbhuanaithe.

Is comhlacht poiblí neamhspleách í an Ghníomhaireacht um Chaomhnú Comhshaoil (EPA) a bunaíodh i mí Iúil 1993 faoin Acht fán nGníomhaireacht um Chaomhnú Comhshaoil 1992. Ó thaobh an Rialtais, is í an Roinn Comhshaoil, Pobal agus Rialtais Áitiúil.

ÁR bhFREAGRACHTAÍ

CEADÚNÚ

Bíonn ceadúnais á n-eisiúint againn i gcomhair na nithe seo a leanas chun a chinntiú nach mbíonn astuithe uathu ag cur sláinte an phobail ná an comhshaol i mbaol:

- áiseanna dramhaíola (m.sh., líonadh talún, loisceoirí, stáisiúin aistrithe dramhaíola);
- gníomhaíochtaí tionsclaíocha ar scála mór (m.sh., déantúsaíocht cógaisíochta, déantúsaíocht stroighne, stáisiúin chumhachta);
- diantalmhaíocht;
- úsáid faoi shrian agus scaoileadh smachtaithe Orgánach Géinathraithe (GMO);
- mór-áiseanna stórais peitreail;
- scardadh dramhuisce;
- dumpáil mara.

FEIDHMIÚ COMHSHAOIL NÁISIÚNTA

- Stiúradh os cionn 2,000 iniúchadh agus cigireacht de áiseanna a fuair ceadúnas ón nGníomhaireacht gach bliain
- Maoirsiú freagrachtaí cosanta comhshaoil údarás áitiúla thar sé earnáil - aer, fuaim, dramhaíl, dramhuisce agus caighdeán uisce
- Obair le húdaráis áitiúla agus leis na Gardaí chun stop a chur le gníomhaíocht mhídhleathach dramhaíola trí comhordú a dhéanamh ar líonra forfheidhmithe náisiúnta, díriú isteach ar chiontóirí, stiúradh fiosrúcháin agus maoirsiú leigheas na bhfadhbanna.
- An dlí a chur orthu siúd a bhriseann dlí comhshaoil agus a dhéanann dochar don chomhshaol mar thoradh ar a ngníomhaíochtaí.

MONATÓIREACHT, ANAILÍS AGUS TUAIRISCIÚ AR AN GCOMHSHAOL

- Monatóireacht ar chaighdeán aeir agus caighdeáin aibhneacha, locha, uiscí taoide agus uiscí talaimh; leibhéil agus sruth aibhneacha a thomhas.
- Tuairisciú neamhspleách chun cabhrú le rialtais náisiúnta agus áitiúla cinntí a dhéanamh.

RIALÚ ASTUITHE GÁIS CEAPTHA TEASA NA HÉIREANN

- Cainníochtú astuithe gáis ceaptha teasa na hÉireann i gcomhthéacs ár dtiomantas Kyoto.
- Cur i bhfeidhm na Treorach um Thrádáil Astuithe, a bhfuil baint aige le hos cionn 100 cuideachta atá ina mór-ghineadóirí dé-ocsaíd charbóin in Éirinn.

TAIGHDE AGUS FORBAIRT COMHSHAOIL

- Taighde ar shaincheisteanna comhshaoil a chomhordú (cosúil le caighdéan aeir agus uisce, athrú aeráide, bithéagsúlacht, teicneolaíochtaí comhshaoil).

MEASÚNÚ STRAITÉISEACH COMHSHAOIL

- Ag déanamh measúnú ar thionchar phleananna agus chláracha ar chomhshaol na hÉireann (cosúil le pleananna bainistíochta dramhaíola agus forbartha).

PLEANÁIL, OIDEACHAS AGUS TREOIR CHOMHSHAOIL

- Treoir a thabhairt don phobal agus do thionscal ar cheisteanna comhshaoil éagsúla (m.sh., iarratais ar cheadúnais, seachaint dramhaíola agus rialacháin chomhshaoil).
- Eolas níos fearr ar an gcomhshaol a scaipeadh (trí cláracha teilifíse comhshaoil agus pacáistí acmhainne do bhunscoileanna agus do mheánscoileanna).

BAINISTÍOCHT DRAMHAÍOLA FHORGHNÍOMHACH

- Cur chun cinn seachaint agus laghdú dramhaíola trí chomhordú An Chláir Náisiúnta um Chosc Dramhaíola, lena n-áirítear cur i bhfeidhm na dTionscnamh Freagrachta Táirgeoirí.
- Cur i bhfeidhm Rialachán ar nós na treoracha maidir le Trealamh Leictreach agus Leictreonach Caite agus le Srianadh Substaintí Guaiseacha agus substaintí a dhéanann ídiú ar an gcrios ózóin.
- Plean Náisiúnta Bainistíochta um Dramhaíl Ghuaiseach a fhorbairt chun dramhaíl ghuaiseach a sheachaint agus a bhainistiú.

STRUCHTÚR NA GNÍOMHAIREACHTA

Bunaíodh an Ghníomhaireacht i 1993 chun comhshaol na hÉireann a chosaint. Tá an eagraíocht á bhainistiú ag Bord lánaimseartha, ar a bhfuil Príomhstiúrthóir agus ceithre Stiúrthóir.

Tá obair na Gníomhaireachta ar siúl trí ceithre Oifig:

- An Oifig Aeráide, Ceadúnaithe agus Úsáide Acmhainní
- An Oifig um Fhorfheidhmiúchán Comhshaoil
- An Oifig um Measúnacht Comhshaoil
- An Oifig Cumarsáide agus Seirbhísí Corparáide

Tá Coiste Comhairleach ag an nGníomhaireacht le cabhrú léi. Tá dáréag ball air agus tagann siad le chéile cúpla uair in aghaidh na bliana le plé a dhéanamh ar cheisteanna ar ábhar imní iad agus le comhairle a thabhairt don Bhord.

Science, Technology, Research and Innovation for the Environment (STRIVE) 2007-2013

The Science, Technology, Research and Innovation for the Environment (STRIVE) programme covers the period 2007 to 2013.

The programme comprises three key measures: Sustainable Development, Cleaner Production and Environmental Technologies, and A Healthy Environment; together with two supporting measures: EPA Environmental Research Centre (ERC) and Capacity & Capability Building. The seven principal thematic areas for the programme are Climate Change; Waste, Resource Management and Chemicals; Water Quality and the Aquatic Environment; Air Quality, Atmospheric Deposition and Noise; Impacts on Biodiversity; Soils and Land-use; and Socio-economic Considerations. In addition, other emerging issues will be addressed as the need arises.

The funding for the programme (approximately €100 million) comes from the Environmental Research Sub-Programme of the National Development Plan (NDP), the Inter-Departmental Committee for the Strategy for Science, Technology and Innovation (IDC-SSTI); and EPA core funding and co-funding by economic sectors.

The EPA has a statutory role to co-ordinate environmental research in Ireland and is organising and administering the STRIVE programme on behalf of the Department of the Environment, Heritage and Local Government.

Environmental Protection Agency
An Ghníomhaireacht um Chaomhnú Comhshaoil

ENVIRONMENTAL PROTECTION AGENCY
PO Box 3000, Johnstown Castle Estate, Co. Wexford, Ireland
t 053 916 0600 f 053 916 0699
LoCall 1890 33 55 99
e info@epa.ie w http://www.epa.ie

SSTI
Strategy for Science, Technology and Innovation

Comhshaol, Pobal agus Rialtas Áitiúil
Environment, Community and Local Government